Development of an Obstacle Detection System for Human Supervisory Control of a UAV in Urban Environments

Andrew Alan Culhane

Thesis submitted to the faculty of the Virginia Polytechnic Institute and State University in partial fulfillment of the requirements for the degree of

Master of Science

In

Mechanical Engineering

Dr. Kevin Kochersberger

Dept. of Mechanical Engineering, Virginia Tech

Dr. Jacob Crandall

Dept. of Aeronautics and Astronautics, Massachusetts Institute of Technology

Dr. Charles Reinholtz

Dept. of Mechanical, Civil & Engineering Sciences, Embry Riddle Aeronautical University

Dr. Alfred Wicks

Dept. of Mechanical Engineering, Virginia Tech

December 4, 2007

Blacksburg, Virginia

Keywords: UAV, Supervisory Control, Obstacle Detection, User Performance Evaluation

Development of an Obstacle Detection System for Human Supervisory Control of a UAV in Urban Environments

Andrew Alan Culhane

ABSTRACT

In order to operate UAVs under human supervisory control in more complex arenas such as urban environments, an obstacle detection system is a requirement to achieve safe navigation. The development of a system capable of meeting these requirements is presented. The first stage of development was sensor selection and initial testing. After this, the sensor was combined with a servomotor to allow it to rotate and provide obstacle detection coverage in front, below, and to both sides of the UAV. Utilizing a PC-104 single board computer running LabView Real-time for on-board control of the sensor and servomotor, a stand alone obstacle detection system was developed meeting the requirements of light weight, low power, and small size. The detection performance of the system for several parameters has been fully characterized. A human subjects study was conducted to assess the any advantages resulting from the addition of the obstacle detection system compared to that of a normal nadir camera. The study demonstrated that users with access to the three-dimensional display were able to navigate an obstacle course with greater success than those with only a camera. Additional development into more advanced visualization of the environment has potential to increase effectiveness of this obstacle detection system.

Acknowledgements

I would first like to thank those who have served as my advisors and mentors in my experiences with unmanned systems and research here at Virginia Tech. Beginning as an undergraduate, Dr. Charles Reinholtz and Dr. Alfred Wicks provided opportunities in unmanned systems which would serve as my motivation for future studies. As a practical researcher, Dr. Kevin Kochersberger has provided additional inspiration for research and has been a source of continuing opportunities to grow as a graduate student. This research would not have been possible without his guidance and efforts to advance the unmanned systems program here at Virginia Tech.

Additionally, I would like to thank my colleagues at the Unmanned Systems Lab at Virginia Tech. Adam Sharkasi, John Bird and all the others who have worked with me over the last two and a half years have all helped to advance my research and help me achieve this goal. Without the knowledge and friendship provided by this group, my research would not have been possible. I also have to thank the Autonomous Aerial Vehicle Team for their hard work to keep our UAVs flying and support my tests. No test flights would have been possible without the help of the piloting skills of Shane Barnett and Prather Lanier.

This research was supported by John Smart at Pacific Northwest National Labs. Thanks to his support and confidence in the unmanned systems lab at Virginia Tech, I was able to develop this system. Dr. Andrew Kurdila has also provided support of this project through the use of hardware and space at the Unmanned Systems Lab. I would also like to thank the Engineering Education Department at Virginia Tech for allowing me to use the SR-20 UAV for this research.

Finally, I would like to thank my family for their support throughout my academic career. Without their help, support, and relentless nagging, I would not have been able to achieve this goal.

Contents

List of Figures

List of Tables

Chapter 1: Introduction

The goal of this research is to create an optimal Obstacle Detection and Avoidance System for a small Vertical take-off and landing (VTOL) unmanned aerial vehicle (UAV) in Urban Environments. The focus of the research can be divided into two parts. The first part of this research is the development of the detection and avoidance system. First, it is important to look at the available sensing technologies and how they have been used on unmanned aerial vehicles in the past so that a good choice can be made. Once a candidate sensor is selected, the next task to evaluate the two-dimensional and three-dimensional capabilities for detecting obstacles.

The second part of the research is the ground station that displays the scene information gathered by the sensor. The goal is to provide the ground station operator with a display that allows for effective human supervisory control of the UAV. In this application, human supervisory control is the process by which a human operator interacts with a computer, receives feedback from the sensors on the vehicle and provides commands to the vehicle [1]. In our case, this refers to commanding a small semi-autonomous helicopter based UAV in an obstacle-rich environment. This concept is also displayed below in Figure 1.1, where the human operator would be at the UAV ground station computer, the onboard flight controller handles the conversion between commands and the actuation of the vehicle, and the task is to avoid obstacles while achieving a mission goal. User performance will be used to evaluate the display effectiveness. Ultimately, the purpose of the research is to demonstrate in-flight obstacle detection and avoidance capability.

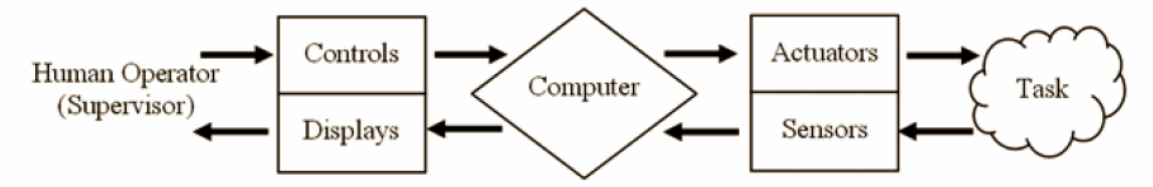

Figure 1.1. Human Supervisory Control [1]

1.1. Motivation and Customer Requirements

As the flight capabilities of unmanned aerial vehicles have increased in recent years, it has become necessary to expand the range of operational conditions in which the vehicle can be used. More specifically, it is desirable to have the use of UAV's in urban type landscapes. In this arena, it is necessary to successfully navigate over and around a variety of different types of obstacles, from buildings to power lines. In post disaster urban environments, this becomes even more challenging because common reference points may have been destroyed making navigation and decision making even more difficult for a UAV operator. The development of this system is focused on improving user performance in navigating these urban environments by accurately detecting obstacles surrounding the UAV as well as displaying this information in an effective, user-friendly manner.

The sponsor of this research has defined several constraints regarding the obstacle detection system. The first set of these restrictions are the power, size and weight restrictions. Because the final UAV for this project is unknown, it is desired that the payload be as light and small, and that it be as low power and low cost as possible. The only one of those requirements that is fixed is the weight, requiring that the entire system weigh less than five pounds. By designing this system to fit and operate on a small UAV, it should have no problems being adapted to fit on a larger UAV in the future. Additionally, at the request of the sponsor, the system must display the scene information in a way that allows an operator to successfully identify and navigate the UAV in an urban environment. The vertical take off and landing ability of the UAV allows for additional degrees of freedom in navigation, and these must be taken into account when choosing a sensor and designing the system.

1.2. Review of Sensing Technologies

To develop the best possible solution to the problem stated above, it is first necessary to understand all available technologies that satisfy the criteria. The following subsections will outline some of the current sensing technologies and how they could be used to accomplish the task of obstacle detection. Technologies where no current sensor is available at this time will not be investigated further. Additionally, only commercially available sensors will be discussed that are within the budget of the research. The scope of this project excludes extensive sensor development at this stage.

1.2.1. LIDAR

LIDAR, or light detection and ranging, is a common measurement technique based on time of flight measurements. In most of the commercially available sensors, a class 1, eye-safe laser in the visible to infrared range is emitted from the sensor, and the time of flight is calculated. Several factors can influence the accuracy of the distance measurement. Because the measurement is based on reflected light, mirrored or transparent objects can cause problems in obtaining valid distance measurements. Also, smoke or fog would pose problems for a LIDAR sensor and reduce the accuracy of validity of distance measurements.

For the purposes of obstacle detection, single point LIDAR units would not provide the spatial resolution necessary to identify obstacles surrounding the UAV. Two-dimensional scanning LIDAR units are available from companies such as SICK AG, Hokuyo and IBEO. These sensors all vary in size and weight, but the functionality between them is similar. Encoded rotating mirrors are used to scan the laser and create a plane of measurements. Angular resolutions vary between sensors, but are usually on the range of half a degree or less. Many of the commercially available products in this class of sensors cannot be considered due to size, weight and power constraints. The most common of these sensors seen in published research is the SICK LMS; however this LIDAR unit weighs almost 10 pounds and consumes 20 Watts of power. The Hokuyo URG is the only commercially available two-dimensional LIDAR sensor that meets the

weight requirements as well as the power, less than a pound and 2 Watts respectively, but does not provide as much range as might be desired: only 5.5 meters. The scanning LIDAR systems cost anywhere from $2,000 up to $70,000 and more.

In order to turn any of these two-dimensional sensors into a system capable of detecting obstacles in all directions around the UAV, additional hardware would be required to rotate the LIDAR to give the desired coverage. This could be accomplished by rotating the sensor itself or potentially by redirecting the laser, which would be significantly more complex.

1.2.2. Radar

Radar is another type of active range measurement sensor based on time of flight measurements. Unlike LIDAR, which uses light, or SONAR, which uses sound, radar uses electromagnetic waves to determine the distance to objects. For the purpose of static ranging, only the time of flight radar units will be evaluated and those using Doppler shift to determine velocities will be ignored. The most common use of Radar units in UAVs has been for altimetry. Radar units such as the Mk V Radar Altimeter produced by Roke Manor Research, and seen in Figure 1.2 mounted on a Yamaha R-Max, have been used to accurately measure the height above ground level for many UAVs. The sensors claim accuracies of 2 cm up to a range of 100 meters with a 10 Hz update rate. These sensors are also much more expensive than similar technologies, and can cost as much as $5,000 for an altimeter unit. One benefit to radar is that it will work through smoke and fog. This is due to the wavelengths used for radar technology. Although this technology would help to identify the nearest target below a UAV, would not provide the spatial resolution necessary to satisfy the customer requirements.

Figure 1.2. Mk V Radar Altimeter Mounted on the Tail of a Yamaha R-Max

Commercial products such as the Honeywell Synthetic Aperture Radar for UAVs would be more suited for obstacle detection. They claim enhanced capabilities for situational awareness and the ability to detect $1m^2$ obstacles at 10 km. They also claim 360 degree azimuth coverage with +/- 20 degree elevation coverage. Although this sensor has the potential for urban obstacle detection, the total weight of 12 pounds and its typical 75 watt power consumption eliminate it from consideration for the current task. Another similar product has been created at Sandia National Laboratories. The miniSAR is a 27 pound synthetic aperture radar claiming 4 inch resolution and a range of 10 km. The miniSAR requires 28 volts and has a 300 watt maximum power requirement. This large power draw eliminates this technology from consideration at this time.

1.2.3. Computer Vision

The main challenge in using computer vision systems for obstacle detection is the distance ambiguity in a single image. A single camera view forces operators to attempt to understand the environment through a “soda straw” or “keyhole” view, making it difficult to determine proximity to obstacles [2-4]. Two of the more common solutions to this problem are single and multiple camera systems. While the hardware, software and motion requirements for both systems are different, they both rely on similar principles of tracking differences between images or frames and using known geometry to calculate

the geometry of the objects in the image. These systems are typically light weight--less than a pound--and can be extremely compact.

In the single camera systems, motion or displacement of the vehicle or camera is required to create this difference between images that is required for image geometry. This technique, known as optic flow, uses feature point tracking to identify similar features in both images and to determine their relative motions between frames [5]. From this data, it derives geometry of objects in the image. Although this method requires very little hardware-just a single camera-the algorithms are very computationally intensive and typically track only a limited number of feature points. The more features that are tracked, the more computationally intensive the process is. Additionally, the distance between images must be known to a high accuracy to avoid large errors in the three dimensional accuracy of objects in the image frame.

Multiple camera systems, such as the Bumblebee2 system made by Point Grey Research Inc. and seen below in Figure 1.3, use a known distance between the two cameras to determine the geometry. This system begins by rectifying the images to adjust the image planes to parallel planes, taking into account the orientation and location of cameras and makes correlation of pixels much less computationally intensive. Algorithms such as the sum of absolute differences or the sum of squared differences are used to calculate the pixel displacement between the two images and then geometry is calculated for all tracked features in the image [6]. The stereo vision method requires less computation and no vehicle or camera movement. Additionally, the images can be collected at rates as high as 48 frames per second at a resolution of 640x480 and the spatial data is collected almost instantaneously.

Figure 1.3. Bumblebee2 Stereo Vision Camera made by Point Grey Research Inc. [7]

One benefit of vision systems, as mentioned above, is the instantaneous nature of the data collection. Unlike the scanning LIDAR or Radar systems, all points in the image are captured simultaneously eliminating error from helicopter drift during a scan. The field of view of these systems is dependent on the type of lens used, and can be as wide as 190 degrees. A limitation of this technology is the reliance on lighting and contrast in images. All of the vision algorithms mentioned require differences between images to find features and generate geometry, making their accuracy highly dependent on the operating conditions of the system.

1.2.4. Ultrasound and Infrared

Ultrasonic and Infrared sensors work on the same time of flight principles as LIDAR and radar. In contrast to those sensors, Ultrasound and Infrared sensors are available at relatively low cost--less than $30--and light weight--less than 0.05 pounds. They are also low power consumption devices, on the range of 75mW. There are two main performance differences between these types of sensors and the previously mentioned LIDAR and Radar sensors: the range and the beam pattern. While some radar and LIDAR units can measure distances on the order of 100 meters and up, infrared and ultrasound sensors are limited to a range of three to six meters. Additionally, both sensors have beam patterns, such as the one seen below for the Devantech SRF08 Range Finder, with cones as wide as 30 degrees or more.

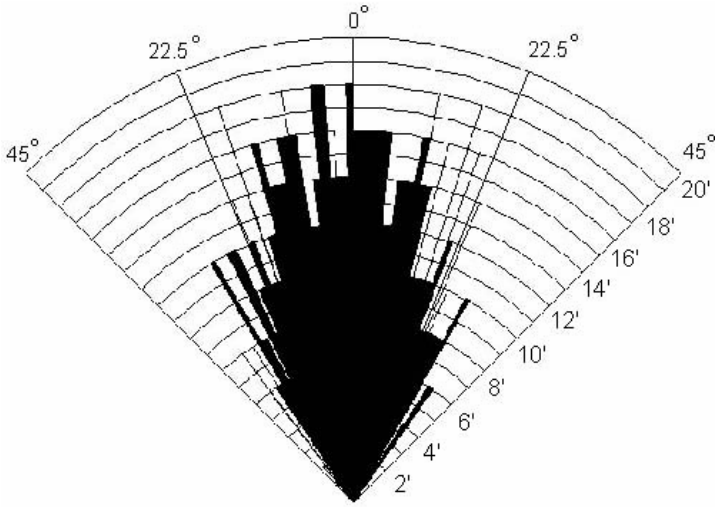

Figure 1.4. Beam Pattern for the Devantech SRF08 Range Finder [8]

Some of the benefits of these sensors include the ability to use several sensors due to their light weight and their low power consumption. One potential issue with adding many of these sensors in a system is cross talk between sensors which may lead to invalid measurements [9]. Proper placement of these sensors could provide total obstacle detection coverage on the same range as a small scanning LIDAR unit; however the spatial resolution would be much lower.

1.3. Current UAV Based Obstacle Detection Systems

The majority of current research efforts in obstacle detection for UAV's can be separated into two categories: Vision and LIDAR based systems. These will be the two initial candidate systems for the obstacle detection system required to satisfy the customer requirements described in the previous section. LIDAR based systems such as those developed at The University of California at Berkley and Carnegie Mellon University have focused on the problems of obstacle avoidance in forward flight. In addition to this, there have been many research efforts using feature point tracking, stereoscopic cameras and optical flow to successfully navigate an urban canyon.

Autonomous Exploration in Unknown Urban Environments for Unmanned Aerial Vehicles [10]

In 2005, researchers at the University of California at Berkley and Seoul National University in Korea presented a paper at the AIAA Guidance, Navigation and Control conference based on navigation of a rotary wing UAV in an urban environment. The paper focused on the two major aspects of exploration in an unknown environment: gathering information about the surrounding of the UAV and avoiding obstacles through path planning. The tests were conducted using an autonomous Yamaha R-Max fitted with a SICK scanning LIDAR unit with an actuated mounting seen below. This system provides obstacle detection coverage from just below to just above the UAV. In testing, the UAV successfully avoided urban obstacles in the form of tent canopies. Avoiding smaller obstacles such as power lines was not tested or discussed in the paper. Additionally, this sensor payload only accounts for obstacles directly in front of the UAV and does not take into account the full range of motion of a rotary wing craft. Payload weight is estimated at 20 pounds based on the SICK scanning LIDAR being the majority of the weight.

Figure 1.5. Sick Scanning LIDAR Unit Mounted on a Berkley R-Max UAV [10]

Flying Fast and Low Among Obstacles [11]

Researchers at Carnegie Mellon University and the University of Southern California published a paper describing a forward flight obstacle detection system and related path planning. The scanning LIDAR system used was developed by FiberTek Inc. with a 30x40 degree field of view in front of the UAV. In this case, a Yamaha R-Max seen in Figure 1.6 was used. This LIDAR system weighs 12 pounds and is capable of detecting power lines and other small obstacles at 100m or more. The obstacle avoidance is a reactive system in addition to a path planning algorithm for successful completion of flight paths. This technology was successfully demonstrated in flight at the McKenna Urban MOUT Site on Ft. Benning, Ga. with forward flight speeds as high as 10m/s. As with the system developed at the University of California, only obstacles in front can be detected with this system.

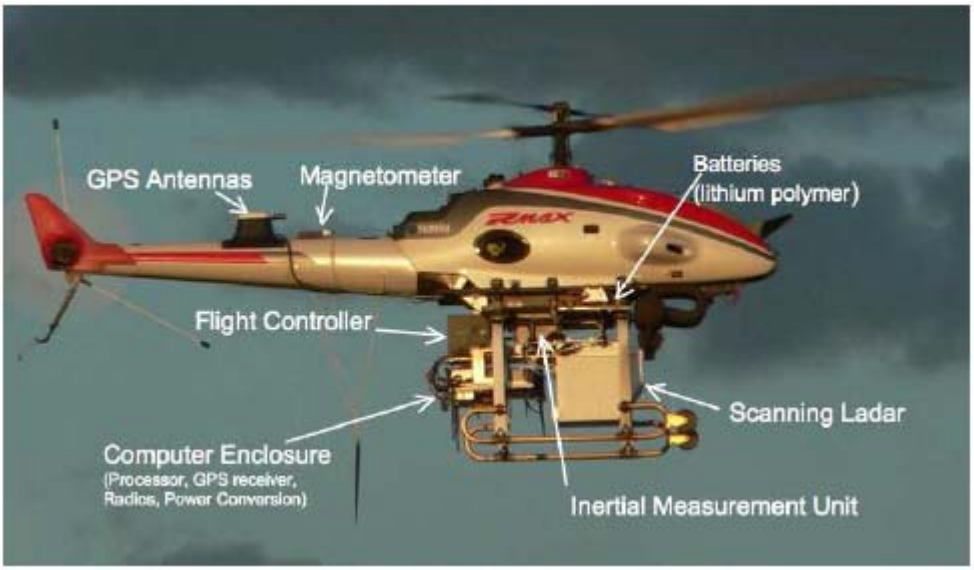

Figure 1.6. CMU R-Max with Fibertek Inc. Scanning LIDAR Onboard [11]

Combined Optic-Flow and Stereo-Based Navigation of Urban Canyons for a UAV [12]

In a paper presented by the University of Southern California and CSIRO ICT Center in Queensland, Australia at the 2005 IEEE International Conference on Intelligent Robots and Systems, a system combining optic-flow and stereoscopic imagery is presented to navigate a small UAV. The platform presented is a Bergen Industrial Twin UAV that uses stereo cameras in combination with fisheye cameras to navigate between buildings and around corners and intersections. The system, seen below, is small and compact, and in tests was successfully able to navigate through urban environments. The system was initially tested on an autonomous tractor to prove the concepts before being deployed n the air. The research focuses on the navigation around large obstacles such as buildings and trees, and does not discuss detecting and avoiding smaller obstacles. The stereo-based system is used for obstacle detection, however this is only forward looking and does not address the additional degrees of mobility available to a rotary wing UAV.

Figure 1.7. USC Avatar platform with Vision System [12]

Chapter 2: Development and Testing of Candidate LIDAR Hardware and Software

The first step in this research was to begin to identify current hardware that could accomplish the task of obstacle detection from a small UAV. A Rotomotion SR-20 UAV was chosen as the platform for system evaluation. The UAV has a total payload of approximately eight pounds. Size and weight were the first two main limitations when looking for an obstacle detection unit. Based on these criteria as well as the technology review in the previous section, a small scanning LIDAR unit was chosen to accomplish this task. Software and hardware development as well as initial sensor testing is described in this chapter.

2.1. Hardware Overview

A Hokuyo URG-04LX 2-D scanning LIDAR unit, seen below in Figure 2.1, was chosen as the main sensor in this obstacle detection payload. This sensor is ideal for the initial system design due to its light weight, small size and low power consumption. This sensor also provides a high scan rate--100ms/scan--and covers a wide area--5.6 meters over 240 degrees. The step size of 0.36 degrees/step is ideal for ensuring detection of small obstacles. Further analysis of the 2-D scanning characteristics of the sensor is shown in the following sections. The full specifications of the sensor are seen below in Table 2.1. It is important to note that this is a class 1 laser that will not cause eye damage.

Figure 2.1. Hokuyo URG-04LX Scanning Laser Range Finder [13]

Table 2.1. Specifications for URG-04LX [13]

Name	Hokuyo URG-04LX
Light Source	Semiconductor laser (785nm) Class 1
Power Requirements	5VDC, 500mA or less
Detectable Distance	0.02 m to 5.6 m
Accuracy	1% of distance
Resolution	1mm
Scanning Angle	240 degrees
Angle Resolution	Approx 0.36 degrees

The sensor handles all of the pre-processing of data internally. Data is returned as distance measurements at each measured angle. This means that distance measurements that return an error are ignored and therefore missing from the final data set. Errors can be returned for measured distances greater than the 5.6 meter range of the sensor, low intensity on reflected light or reading errors due to strong reflective objects. Other error types exist. However the manufacturer does not go into more detail regarding the cause of the measurement error. This internal error handling allows for simplified post processing because only valid distance measurements are returned, which limits the amount of processing and data management required. This also poses problems because obstacles can be missed entirely if there is no valid return off the surface. These issues will be addressed later in this section.

2.2. Software and Electronics Overview

In order to use the URG-04LX, software was written to communicate and parse the data from the sensor. LabView, developed by National Instruments, was used to create the software interface to the sensor using a serial port. Initial software development focused on proper serial commands as specified in the communication guide for the sensor as well as parsing the serial data received from the sensor into meaningful distance and angle measurements. These measurements were then converted into Cartesian coordinates for later analysis.

To transition from a bench top testing system to a deployable payload, several options were considered for control of the sensor. A system was designed using a SBC1589 PC/104 single board computer, seen below in Figure 2.2, running a LabView Real-Time operating system. This system provides an ability to create a stand alone system to control the sensor and transmit the data back to a ground station over Ethernet for post processing and display. The UAV uses an 802.11 Ethernet bridge for communication with the ground station allowing for simple integration of the single board computer with the current on-board hardware. As with the sensor, light weight, small size and low power consumption were requirements for selecting this computer. The board measures 3.55” by 3.775” by 0.6”, weighs approximately 0.25 pounds and draws 0.6 amps at 5 volts.

Figure 2.2. SBC1586 PC/104 Single Board Computer [14]

In addition to the PC/104 computer, a custom power distribution board was designed and built in the Unmanned Systems lab a Plantation Road to provide regulated power to the computer and has additional power available for the sensor. Schematics for this board can be found in Appendix A. The total weight of the computer, power distribution and sensor is slightly less than one pound. This system allows for easy deployment on the UAV due to its light weight and modularity, allowing the sensor and computer to be placed independently.

2.3. Initial Testing and Calibration

To evaluate the LabView code as well as the sensor data being returned, initial testing was conducted on the system. The first of these tests was to place a flat white sheet that was 300mm wide approximately 835mm away from the sensor and parallel to the front of the sensor. The collected data is seen below in Figure 2.3. It can be seen that the width of the object appears to be accurate, however the center is shifted in the negative y direction and the data is not linear in the x values. In order to evaluate the source of this error it necessary to understand how the sensor collects the data.

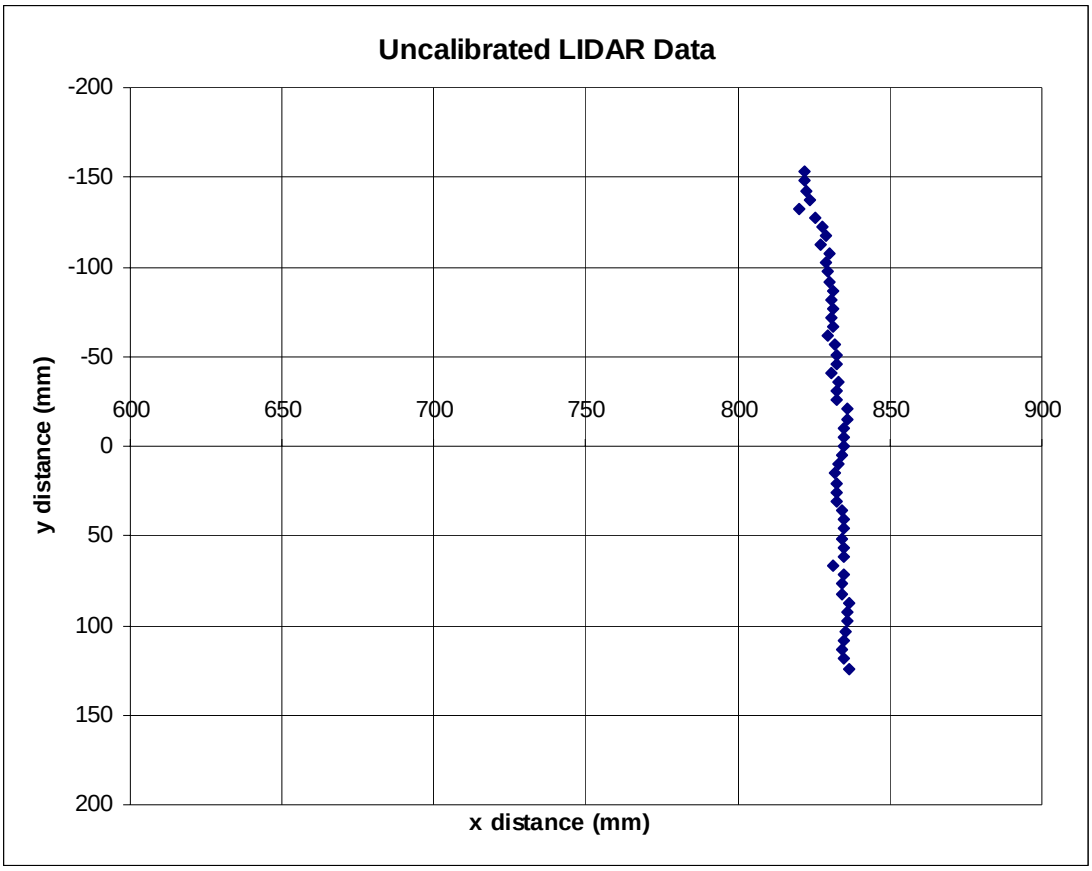

Figure 2.3. Uncalibrated LIDAR Data for a 300mm Object. The LIDAR unit is located at (0,0)

The sensor collects the data in a counterclockwise direction. It returns the data as sequential measured distances which must be correlated to the correct corresponding angle. The equation to calculate this is written in the following way:

$$\theta_{current} = \theta_{initial} + i_d \cdot \theta_{step} \quad (2.1)$$

where $\theta_{current}$ is the corresponding angle for the current distance measurement, $\theta_{initial}$ is the starting angle for distance measurements, i_d is the index value of the distance measurement and θ_{step} is the angle advanced by the sensor between distance measurements. The only potential sources of calibration to correct this error in return measurements would be to adjust $\theta_{initial}$ or θ_{step}. The initial angle is supplied to the sensor in the command to begin the scan and the manufacturer states that $\theta_{step} = 0.3515625^o (360^o / 1024)$. Looking at the data in Figure 2.3, it can be observed that data further into the scan appears more skewed and closer to the sensor. This would be a result of the actual step angle of the sensor being smaller than the $\theta_{step} = 0.3515625^0$ the manufacturer stated. Additionally, the data being shifted slightly in the negative y direction would be a result of the initial angle being slightly different than what was specified. By adjusting these parameters to fit the uncalibrated data to the known distance and obstacle size, a calibrated set of collected data is plotted in Figure 2.4. The data is now centered on the y=0 line with a width in the y direction of near 300mm and appears much less distorted as the scan progresses. Further tests can determine if these distance measurements are within the manufacturer specifications for the accuracy of the sensor.

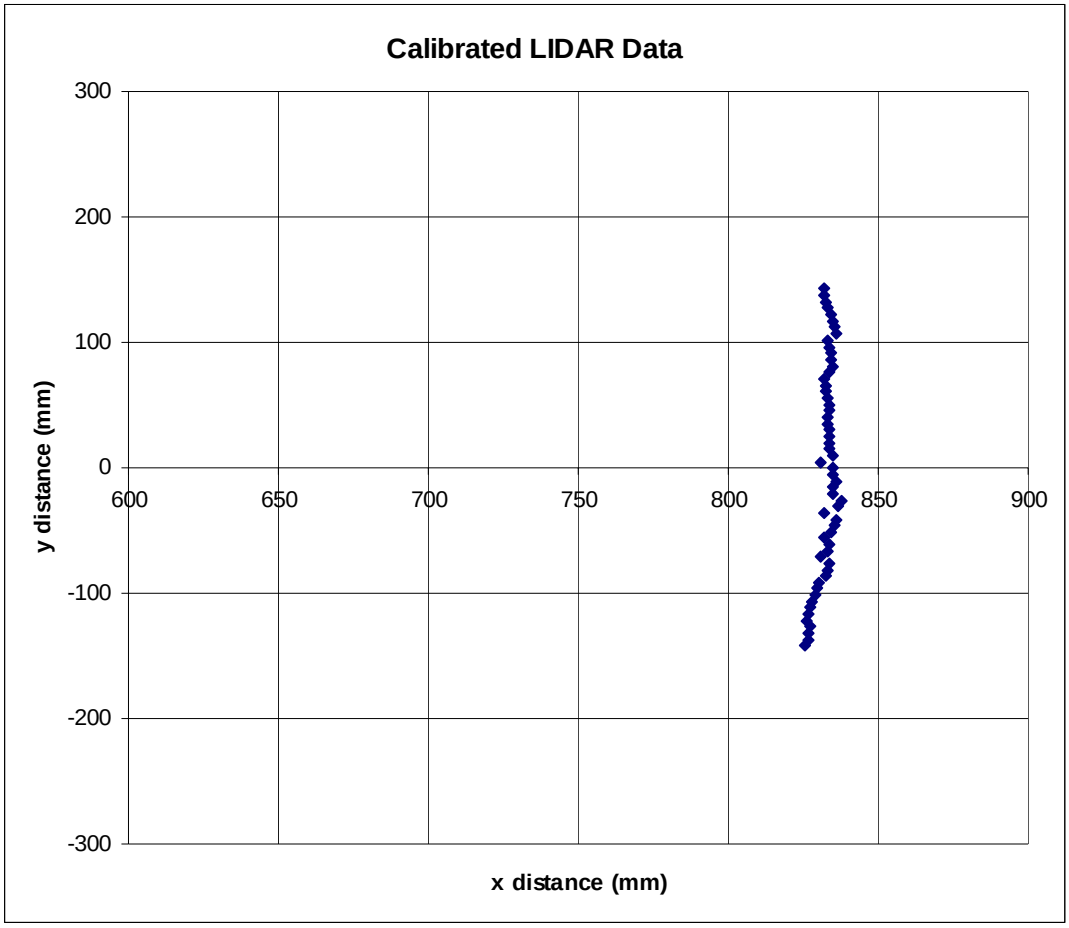

Figure 2.4. Calibrated LIDAR Data Using Correction Factors. The LIDAR unit is located at (0,0)

2.4. Two-Dimensional Sensor Evaluation

With the initial analysis of the system complete, the next step is to characterize the performance of the sensor with regard to the desired obstacles being detected. Although the final goal of this system is obstacle detection in three dimensions, it is first necessary to determine the accuracy and reliability of the sensor in a single plane. Error analysis, tests and data for the two-dimensional performance of the Hokuyo URG-04LX sensor are presented in the following sub-sections.

2.4.1. Two-Dimensional Error Analysis

To properly understand the accuracy of the LIDAR sensor being used and to be in a position to make proper assessments of the actual performance compared to the manufacturers' specifications, it is first necessary to determine how the errors in measured distance affect the perception of objects. As seen in the table of sensor specifications, there is a stated accuracy of 1% of the distance measurements and no information on the accuracy of the step angles inside the sensor. For this reason, the error calculations below will determine the resulting positional errors due to expected errors in distance measurement.

The sensor returns distance and angle measurements. In the equations below, D will represent the distance returned by the sensor and θ_L will represent the internal angle measurement of the LIDAR. The subscript L denotes the LIDAR coordinate frame. The LabView code uses D and θ_L to determine x_L and y_L, the x and y coordinates of points in the LIDAR fixed frame, using these relationships:

$$\begin{aligned} x_L &= D \cdot \cos(\theta_L) \\ y_L &= D \cdot \sin(\theta_L) \end{aligned} \tag{2.2}$$

As stated, the error in distance measurements, D, is 1%, and therefore the error in distance measurements, e_D can be expressed using the following equation:

$$e_D = 0.01D \tag{2.3}$$

By combining the relationship for error in the distance measurements with the equations for the x and y coordinates in the LIDAR fixed frame, equations for error of the x and y coordinates of a point are determined to be as follows:

$$\begin{aligned} e_{x_L} &= 0.01D \cdot \cos(\theta_L) \\ e_{y_L} &= 0.01D \cdot \sin(\theta_L) \end{aligned} \tag{2.4}$$

These equations can be used to determine the maximum expected error in the x and y values of any objects in the LIDAR scan. At noted before, these error equations ignore the potential error in x_L and y_L that would result from errors in θ_L. There is no analytical method available to determine this accuracy.

In addition to the measurement errors due to the error in D, there are also errors in the perceived location and size of objects due to the internal step size of the LIDAR. When determining the width, or size in the y axis, of an object, the expected accuracy is based on the angular resolution of the sensor. The worse case scenario for finding the width of an object would be that the LIDAR measurements just miss detecting each edge of the obstacle, where the first and last measurements are taken one angular step size from each edge, resulting in an object being detected narrower than the actual value. This error is a function of distance, and can be quantified by this equation:

$$e_{y-step} = 0.008 \cdot D \tag{2.5}$$

In this equation e_{y-step} is the maximum expected error in the width measurements and D is the distance to the object from the sensor. This source of error can cause inaccuracies in the perceived width of an object, as well as the perceived center. The perceived center of an object in the y direction can be expected to shift no more than half the expected y error

in either direction. The error equations 2.4 and 2.5 will be verified experimentally in the following sections.

2.4.2. Finding the Lower Limit for Accurately Detecting Obstacles

One of the principle desires for the obstacle detection system is to detect small obstacles such as cables or rebar. In order to characterize these properties, initial calculations were performed using the sensors technical specifications found in Table 2.1 above. By assuming each laser measurement can be approximated as having no width, it is possible to determine the maximum distance between two measurements based on the angular resolution of the sensor. The sensor requires that an object is detected in two consecutive measurements in order to return a valid distance measurement. This requires that an object must be no smaller than the distance between three consecutive measurements. Based on this criteria and the internal step size of the LIDAR, the following equation is found using basic trigonometry:

$$MinObstacle = 0.008 \cdot D \tag{2.6}$$

where D is the range from the sensor. This is identical to equation 2.5 and is based on the same sensor properties of angular resolution. For example, at 1 m away, the smallest obstacle that can be expected to be found with repeatability is 8 mm. This analysis provides an expected value of detectable obstacle sizes to verify experimentally.

To verify this analysis, a series of simple tests were performed to determine the minimum detectable size of an object. Using the derived equation above, objects were selected that correspond to the minimum detectable size at a distance of 1 meter. Starting with the 8 mm object placed in 20 arbitrary locations 0.5 meters from the sensor, statistics for positive detection of the object were generated. The test was repeated, increasing the distance by 0.5 meters until the detection rate dropped below 75% over the 20 scans. The table below shows the results of this test.

Table 2.2. Results of the Test to Determine the Smallest Detectable Object

Distance (meters)	Detection Rate (% of times found)
0.5	100
1	95
1.5	45

From the data, it can be determined that equation 2.6 correctly predicts the smallest detectable object for the sensor. Additionally, because this equation is linear, it scales through the range of the sensor. Therefore, the smallest object that can be confidently identified at the maximum range of 5.5 m has a minimum width of 44 mm. For detecting smaller obstacles in urban environments a LIDAR sensor with a smaller internal step angle would be required. However no sensors were found with this characteristic, which makes this a necessary limitation at this point in the system development.

2.4.3. Effects of Shape and Surface Material on Detection of Obstacles

Another important aspect to evaluate in the performance of the LIDAR sensor is the effect of different shape and material obstacles. These can be evaluated in two separate tests. These tests were limited to shapes and textures found in an urban environment. This helps to identify objects that pose potential detection problems in the common operating environment of the sensor. To evaluate the effect of different textured materials, a baseline test was first conducted to establish accuracy and standard deviation in spatial measurements. An object of known width (y-axis) size was placed at a known distance (x-axis) away from the sensor and covered by a solid white sheet. Distance measurements to the object were sampled 20 times. From this collected data, it is possible to determine the accuracy and repeatability for both the x and y measured directions. The error resulting from equations 2.4 would result in a maximum possible error in the x direction of 1% of the distance measurement, which would be 10 mm. Using the error equations 2.4 and 2.5, it is reasonable to expect errors in the measured width to be, in the worst case, 16 mm. The y position errors due to the equations 2.4 are

ignored because the distance error effects are less than 0.4 mm given the location of the measured object.

The results of this test show that for an object placed at 1 meter, the accuracy in the distance measurement was 0.92 %, slightly higher than the claimed distance accuracy with a standard deviation of 3 mm. The sensor was only able to determine the horizontal size of the object within 8.4% of the actual size, finding it 25 mm smaller than the true size in all tests. This measurement also had a standard deviation of 3.3 mm. This larger than predicted measurement error in the horizontal size of the object may be attributed to a lack of valid data returned at the edges of the object. As stated above, the sensor does not return a distance measurement if a valid return is not received by the LIDAR unit.

Using the same method as the previous test, several other objects of the same size and shape were placed at the same distance away and measured. Similar measurement statistics were generated and appear in the table below. Surface types measured were the white sheet, a black sheet, a metallic surface and wood. All objects were placed 1 meter away from the sensor and had a width of 300mm.

Table 2.3. Measurement Statistics for Different Surface Types

Surface	Average distance (mm)	Distance Accuracy	Distance S.D.	Average Width (mm)	Width Accuracy	Width S.D.
White Sheet	1009	0.92%	3.3	275	8.40%	2.5
Black Sheet	988	1.10%	17.1	268	10.60%	10.2
Metallic	996	0.79%	20.1	267	10.80%	8.7
Wood	1002	0.30%	3.6	287	4.30%	0.41

This test verifies the manufacturers stated accuracy of the sensor as well as shows some other important characteristics of the sensor. Surface material does not appear to make any significant difference in the average distance of the object, but in the case of the metallic and black surfaces, the standard deviation of those results is much higher than the wood or the white sheet. Although the distance of the object is not found consistently, the object is clearly detected and the average distance is within the expected

values. Because the goal of this system is to detect obstacles near the UAV and not high precision geo-referencing, the variation in the width measurements is acceptable for this application.

When characterizing how different shapes affect the distance information, the main concern is the effect of obstacles, or portions of obstacles, at sharp angles from the sensor. This gives the potential for the laser to be reflected away from the sensor and return no measurement. To test this, two objects, one a matte white poster board cutout and the other a non polished aluminum plate, each 0.25 m in length will be placed 0.5 m away from the front face of the sensor. The obstacles will start parallel to the front face of the sensor, and then will be rotated up to 90 degrees, or less if no valid data is returned. The goal here is to determine when the sensor can no longer identify the object due to the angle of rotation.

Through testing, it was determined that the white sheet will always be identified until the visible width of the sheet is less than the minimum detectable object as calculated above. In the case of the metallic surface, which was a clean piece of sheet aluminum, the sheet was detected until the angle reached 87 degrees away from parallel. In this case, the visible width of the sheet was still larger than the minimum detectable obstacle at 0.5 m. A more polished metallic surface may have caused detection issues at less of an angle, but this material was chosen to more accurately represent potential obstacles as they were laid out in the mission specifications.

2.5. Three-Dimensional System Evaluation

After characterizing the two-dimensional performance of the LIDAR sensor, the next step in this research was to create a system capable of three-dimensional scans covering a hemisphere centered below the UAV. Ideally, a system would be capable of collecting obstacle data in front, below, on either side and behind the vehicle. This would allow for sufficient scene information to allow an operator to identify obstacles in most of the degrees of freedom on the UAV. The process of designing and testing this system is described in the following section.

2.5.1. Hardware and Software Overview

To develop a system capable of taking a two-dimensional distance measurement sensor and generating three-dimensional data sets, one would need an actuator that has the ability to accurately rotate the sensor through a minimum of 90 degrees for initial concept development. Several concepts using different mounting schemes and different motors were investigated, finally leading to the initial concept using a servomotor in combination with a controller board. The servomotor is a high-torque model manufactured by HITEC and the controller board is the SV203 manufactured by Pontech. In combination with gears, an external potentiometer and the controller board, the motor is capable of rotating the LIDAR unit 130 degrees with 0.9 degree resolution. The servomotor, sensor mount and LIDAR sensor can be seen below in Figure 2.5. The added components add 1.1 pounds to the weight of the system, with the total system weighing 2 pounds.

Figure 2.5. Servomotor, Sensor Mount and LIDAR Sensor

One important consideration in choosing the servomotor was how it would interface with the current system using the PC-104 single board computer and LabView RT described in the previous section. This is accomplished by sending serial commands to the controller board from the single board computer. Initially, software was written to simply control the servomotor accurately in LabView, and once this was accomplished, the next step was to integrate the LIDAR and motor control software into one program. Timing was the first consideration in this process. The servo control is an open loop process, where angles are given, but no feedback is received if the position was changed. This causes an issue with timing the servo movement with the LIDAR scan to correctly correlate the two-dimensional data to three-dimensional coordinates based on the angle of rotation of the sensor. After accounting for this timing issue as well as integrating the LIDAR and servomotor software, a final set of code was generated that would initialize a 3-D scan, rotate through variable angular steps, and return x, y and z coordinates properly rotated to the vehicles coordinate system. The process of rotating the scan data to the

vehicles coordinate frame is done as a single axis rotation about the y-axis of the scanning unit, resulting in these equations:

$$\begin{aligned} x_B &= x_L \cos(\theta_S) \\ y_B &= y_L \\ z_B &= z_L \sin(\theta_S) \end{aligned} \tag{2.6}$$

The subscript B denotes the body frame of the UAV; L denotes the LIDAR frame; θ_S is the angle of rotation due to the servomotor. Because the scanning system will be mounted near the center of the UAV the translation in the x and z directions is ignored. This data is then sent back to the ground station using shared variables in LabView and used to generate the obstacle display. In order to verify that the data was being collected, properly rotated and displayed correctly on the ground station, several static scenes were scanned and obstacle maps generated. Below is a picture of one of the test scenes; a pole leaning against a wall. This scene was scanned with the obstacle detection system and displayed on the ground station. Test scenarios such as this were used initially to qualitatively verify proper operation of the system. A more quantitative, in depth analysis is done in the following sections.

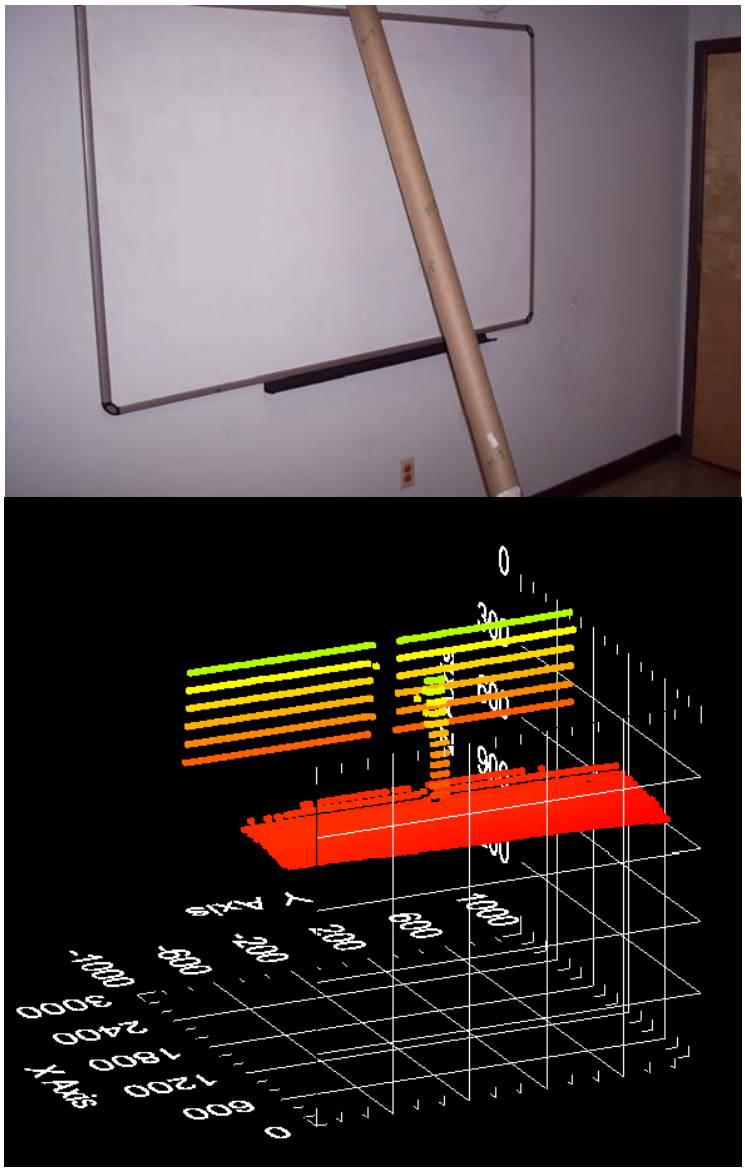

Figure 2.6. Comparison of Photograph and LIDAR Scan Data of a Pole

2.5.2. Three-Dimensional Error Analysis

After developing a working combination of servomotor and LIDAR unit, the next step in the analysis of the full obstacle detection system is to determine how the two-dimensional errors couple with the three-dimensional rotation as well as any new sources of error in obstacle detection that have been introduced. Similar to the issues in characterizing the errors due to internal step angle of the LIDAR sensor, there is no available data on the accuracy of the servomotor used to rotate the sensor. For this

reason, this is ignored at this time. This assumption will be verified through testing. The errors caused in three-dimensional space due to the single axis rotation about the y axis of the LIDAR coordinate frame are found by propagating the x and y error values from the LIDAR frame through the rotation and ending up in the body frame of the UAV. Using the equation 2.4 for e_{X_L} and e_{Y_L}, substituting into the single axis rotation equations 2.6, the three-dimensional error equations can be written the following way:

$$\begin{aligned} e_{X_B} &= e_{X_L}\cos(\theta_S) \\ e_{Y_B} &= e_{Y_L} \\ e_{Z_B} &= e_{X_L}\sin(\theta_S) \end{aligned} \tag{2.7}$$

Where the subscript L indicates the LIDAR coordinate system and B represents the standard body coordinate system for an aerial vehicle. Substituting gives these final equations of:

$$\begin{aligned} e_{X_B} &= 0.01D\cdot\cos(\theta_L)\cdot\cos(\theta_S) \\ e_{Y_B} &= 0.01D\cdot\sin(\theta_L) \\ e_{Z_B} &= 0.01D\cdot\cos(\theta_L)\cdot\sin(\theta_S) \end{aligned} \tag{2.8}$$

These errors quantify the error of a single x, y, z point in the body frame of the UAV due to the accuracy error in distance measurements only for the LIDAR sensor.

To quantify the errors resulting from the servomotor system used to rotate the sensor, error from the step size of the rotation--similar to the error mentioned above for the width of an object--must be characterized. The error resulting from step size is similar to equation 2.5 above relating to the minimum detectable obstacle to the distance away, but similar to the worst case scenario for width measurements above, the maximum expected error in the height, or x direction, of on obstacle can be defined as this:

$$e_{X-Step} = 0.02 \cdot D \cdot StepIncrement \quad (2.9)$$

The e_{X-Step} is the maximum expected height error, D is the distance from the sensor and StepIncrement is the number of servomotor steps taken per LIDAR scan. Again this error can result in a perceived height detected smaller than the actual value as well as a perceived x center shifted half the expected x error in either direction. These maximum expected error calculations will be used to verify experimental tests later in the chapter.

2.5.3. Comparison of Scanning Speed versus Feature Detection

As mentioned in the previous section, the angular resolution of the servomotor as well as the step size used can affect the accuracy of detecting the size of objects. Additionally, this angle can be used to determine the smallest obstacle that can be reliably detected at different distances. By approximating the scans from the LIDAR to be solid planes, it only requires basic trigonometry to generate an equation to determine the maximum unscanned area in which an object could potentially be missed by the system. Using the same method used to determine equation 2.5 for the smallest detectable object for the LIDAR, the equation is determined to be as follows:

$$MinObstacle = 0.01 * Range * StepIncrement \quad (2.10)$$

In this equation, *MinObstacle* represents the minimum obstacle size that can be reliably detected, *Range* is the distance the obstacle is from the sensor and *StepIncrement* is the step size command given to the motors. The step size given to the motors is an integer number and therefore there are only discrete steps available during the sweep of the sensor. The smallest step size corresponds to approximately a 0.9 degree movement of the sensor.

Due to the fact that this system is used on a hovering UAV in a time critical mission, it is necessary to characterize the relationship between the time it takes for a scan to complete versus the minimum obstacle size. It is a simple process to change the

step size, so this can be an adjustable value depending on the specific mission requirements. Figure 2.7 below show the relationship between then smallest detectable obstacle and the step size while Table 2.4 shows the scan times for each of the step sizes, 1 to 10. The combination of the graph and table below allow a system operator to select the appropriate step size based on the tradeoffs between the allowable scan time and the anticipated obstacle size.

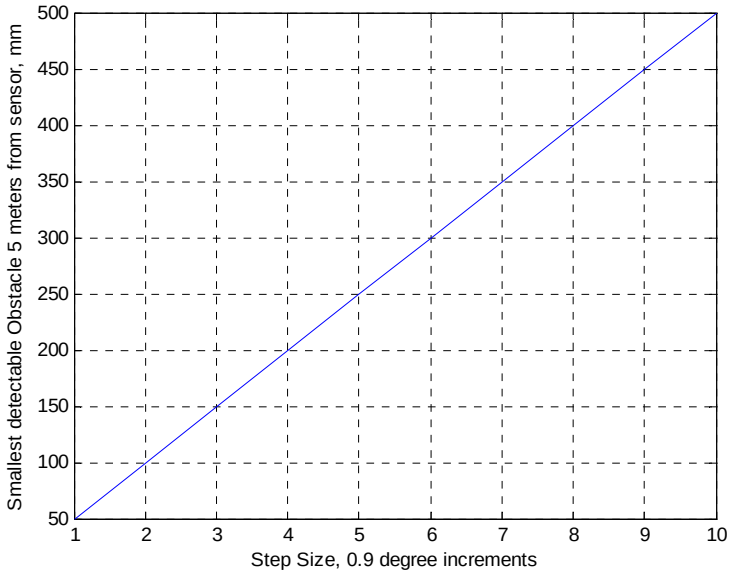

Figure 2.7. Relationship between Servomotor Step Size and the Smallest Detectable Object at 5 meters from the Sensor

Table 2.4. Relationship between the Servomotor Step Size and the Time taken to complete a Three-Dimensional Scan

Step Size	Scan Time (seconds)
1	110
2	60
3	40
4	30
5	23
6	20
7	16
8	14
9	13
10	11

The scan time was measured as the time required to complete the scan and to transmit new data to the ground station. This is affected by step size in two ways. The first is the time is takes the servomotor to sweep the sensor through the 130 degree range stopping to collect data at each step of the scan. The second is the size of the data arrays being sent back to the ground station. Although the first is much more influential to the scan time than the second, they both are factors.

In order to experimentally verify the relationship between step size and smallest detectable obstacles, a step size of 5 was chosen. Using equation 2.10, a 50mm object was selected corresponding to the minimum detectable obstacle at 1 meter from the sensor. This size is much larger than the lower limit of the LIDAR sensor removing the possibility of not detecting the object due to sensor limitations. Similar to the experiment to determine the smallest detectable object for the LIDAR sensor itself, the object was originally located 0.5 meters from the sensor, and moved away until the detection rate dropped below 75% over 20 scans. Table 2.5 shows the results of this test.

Table 2.5. Scan Percentages for 20 LIDAR Scans

Distance (meters)	**Detection Rate (% of times found)**
0.5	100
1	100
1.5	65

2.5.4. Testing System Effectiveness in Three Dimensions

For the test to determine the accuracy of the three-dimensional scanning system, a 330mm by 330mm white plate will be placed 1 meter away. The test will be to locate the center of the plate at what should be the coordinates x=0, y=0 and z=1 as mentioned previously. The measurements will be taken using a servomotor step size of 5. Using equations 2.5 and 2.9, and approximating the distance of the entire plate to be 1 meter from the sensor, the expected error in the width is 8mm and the expected error in the height is 100mm. These errors would also lead to an expected uniform error in the x and

y centers to be 50mm and 4mm respectively. Due to the close range of the obstacle as well as the small scan angles at the edges of the obstacles, the resulting error due to the 1% distance error is less than 1mm for the x and y directions and therefore only considered in the z direction. Data was collected for 10 scans of the obstacle detection unit and then the average x, y and z locations of the plate were calculated as well as the average perceived heights and widths of the plate.

Table 2.6 summarizes the results for the height and width calculations. The measured values are based on the average height determined from the 10 trials. The measured errors for both the height and width fall within the expected values determined by the error equations 2.5 and 2.9. This data helps to verify the theoretical error analysis for perceived obstacle sizes.

Table 2.6. Height and Width Summary Table

Obstacle Size	Height	Width
Expected Value	330	330
Measured Value (averages)	254	322
Expected Error	100	8
Measured Error (averages)	76	8

Using the same data sets that were used above, the perceived location of the measured center of the plate were determined from the average of the 10 scans and summarized in Table 2.7. As stated before, the expected error in the calculated centers is 50mm in x, 4mm in y and 10mm in z. From the measured data, the error in the x location was 35.5mm--less than expected, however errors of 6.4mm in y and 16mm in z were found.

Table 2.7. Summary of the Measured Center of the Obstacle

Location of Center	x	y	z
Expected Value	0	0	1000
Measured Value (averages)	-35.5	-6.2	1016
Expected Error	50	4	10
Measured Error (averages)	35.5	6.2	16

One potential source of this additional error is in the placement of the obstacle and the sensor. With no three-dimensional placement system with a higher accuracy than

the theoretical accuracy of the sensor, determining the actual location of the center of the plate relative to the sensor was a non trivial task. This is the reason the only location tested was directly in front of the sensor. To test additional locations, a high accuracy system would have to be developed with accuracies on the millimeter level would be required. These tests helped to verify the theoretical accuracies of the system, and further testing with more accurate equipment would be required to test additional locations.

2.6. Conclusion of System Performance

Through extensive two-dimensional and three-dimensional system analysis, the performance of LIDAR based obstacle detection payload was determined. The system followed easily predictable performance based on component characteristics of the LIDAR sensor as well as the servomotor. More detailed three-dimensional analysis could be performed in the future, however at this stage of development, the theoretical equations for system error are found to accurately characterize the errors.

The purpose of this system is to accurately represent obstacles surrounding a UAV in an urban environment. Based on the data presented above, an operator can accurately determine desired scan settings based on the predicted scene conditions. All the accuracies of location and perceived size are much smaller than the possible position accuracies of available UAVs and should provide more than sufficient obstacle information. With verified millimeter accuracies in distance measurements, there is the potential for enhancing the system performance to include geo-referencing of obstacle data.

Chapter 3: System Architecture

The systems architecture defines how all systems function together to accomplish sensing and data display to the ground control station operator. Ideally, a good systems architecture is one which optimally uses software and hardware for the mission operation. In this case, this mission has been defined by the sponsor of the research. The overall system consists of the LIDAR system selected and described in the pervious chapter, a UAV to carry the payload and a ground station to display the data and give the operator sufficient data to complete the mission. The defined mission and the system developed to complete this mission are described in this chapter.

3.1. Mission Overview

In addition to the sensor performance requirements set out by the sponsor of this research, a typical mission has also been specified. The UAV would take off under control of a safety pilot and be switched into autonomous mode. At this point, the UAV would travel into an unknown urban environment out of sight of the ground station operator. Higher altitude vision algorithms will be used to select a candidate site for descent into an urban canyon or other similarly challenging area. At this point, a more tactical descent and navigation will begin with the use of the obstacle detection payload combined with the ground station display. The operator will be expected to successfully navigate around buildings, power lines, trees and other common obstacles. Due to limited flight times, speed in navigation is critical and therefore the system must be capable of detecting obstacles in a timely manner and displaying this to the UAV operator. Tactical navigation will be achieved using relative translation commands rather than GPS points because the scene information from the sensor is locally referenced to the UAV and not geo-referenced. This would require the use of inertial and GPS data from the UAV and increases the computational complexity of the system greatly.

3.2. System Overview

The overall system being used to evaluate the UAV-based obstacle detection and avoidance payload consist of three parts. The first part is the payload itself, which has been described in depth in the previous sections. The next part is the UAV that will fly with the payload on it and will serve as the vehicle that performs the navigation. The last component of this system is the ground station. This provides the user interface that allows the UAV operator to interpret the sensor data and make proper navigation decisions. Each component of the system will be described in detail in the following section. Additionally, a full explanation of the safety procedures and system operation for flight testing is provided.

3.2.1. Overview of the SR-20 platform

The SR-20 autonomous helicopter is a Rotomotion LLC product that sells for approximately $16,000 and includes the flight controller hardware and software. It is a VTOL UAV based on an ION X-Cell RC helicopter adapted with the Rotomotion autonomous flight control system (AFCS). The system uses two 5-cell lithium ion batteries to power a 1300W electric motor capable of lifting an additional 8 pounds of payload. The UAV uses 802.11-based telemetry, which is currently handled using a MOXA AWK-1100 wireless bridge. In addition to the flight controller and the wireless bridge, the SR-20 used for these tests was equipped with a 5-port Ethernet switch as well as an AXIS 206 network camera. The SR-20, before the addition of the obstacle detection system, can be seen below in figure 3.1. In addition to the two main lithium ion batteries to power the electric motor, a 3-cell battery powers the AFCS and the Ethernet switch, and a 4-cell battery powers the wireless bridge. In this configuration, the flight time is approximately 15 minutes, with the limiting factor being the motor batteries. With the additional hardware required for the obstacle detection, it is estimated that the flight time will decrease to around 10 minutes; however this has never been tested for safety reasons. Rotomotion claims that in a hover, the UAV has a hover hold accuracy of less than two meters and an altitude hold accuracy of less than 0.5 meters in a light wind. Due to the

small size of the SR-20, it is more affected by wind gusts compared to heavier helicopters. Deviations of 5 meters or more have been seen when testing in gusty conditions.

Figure 3.1. Rotomotion SR-20 VTOL UAV [15]

3.2.2. Mounting and Static Testing of the Obstacle Detection System

Several things were taken into consideration when mounting the obstacle detection system on the SR-20. The first of these was sensor placement. Ideally, the sensor would be directly under the center of the UAV for maximum coverage. Unfortunately, that is also the location of the flight controller. The next best available mounting point is just in front of the flight controller, centered on the x axis of the UAV and near the bottom of the landing gear. The mounting location can be seen below in Figure 3.2. This allows for clear forward and downward sensor coverage with no obstructions. This also allows for a place to mount the nadir looking camera seen next to the LIDAR sensor. In this orientation, the sensor will see the landing gear and some of the other parts of the UAV. However, it is possible to filter these out. Due to the modular nature of the system, the single board computer, servo controller and power distribution

can be mounted away from the LIDAR and camera. Because of space restrictions, the only place this can be mounted is on the front of the UAV. This does place it near the LIDAR and camera for easy wiring.

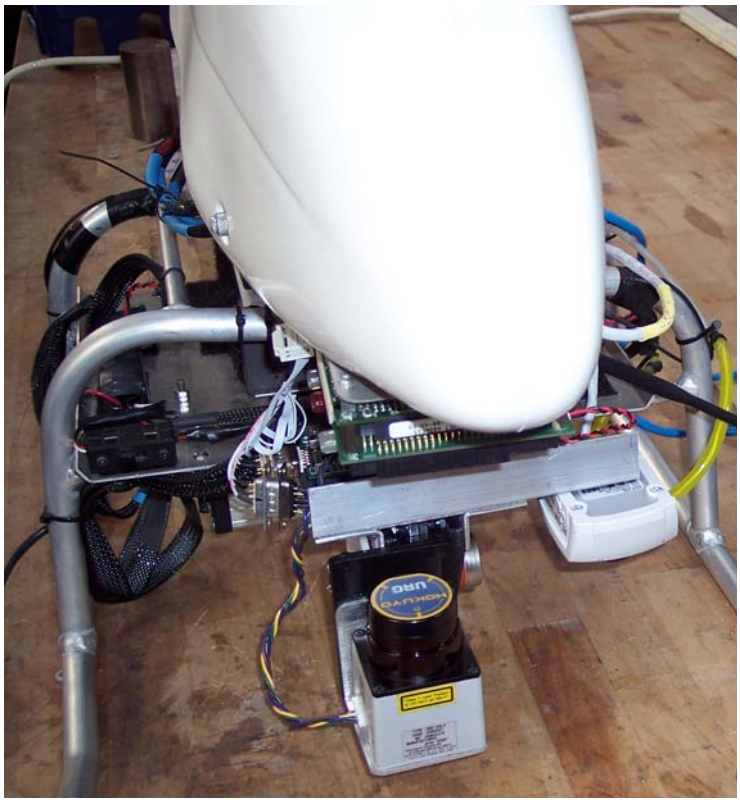

Figure 3.2. Mounting of Obstacle Detection System Components on the SR-20.

Due to the potential for high vibration on the platform, it is important to isolate these components from the airframe and the engine. The UAV comes from Rotomotion with the landing gear vibration isolated from the body of the helicopter using small rubber dampers seen in Figure 3.3. This fact is taken advantage of by mounting the LIDAR unit to the landing gear tray. Also, the single board computer and power distribution are also isolated separately seen in Figure 3.4. Both of the isolation schemes are seen below. The IMU inside the AFCS verifies the vibration isolation.

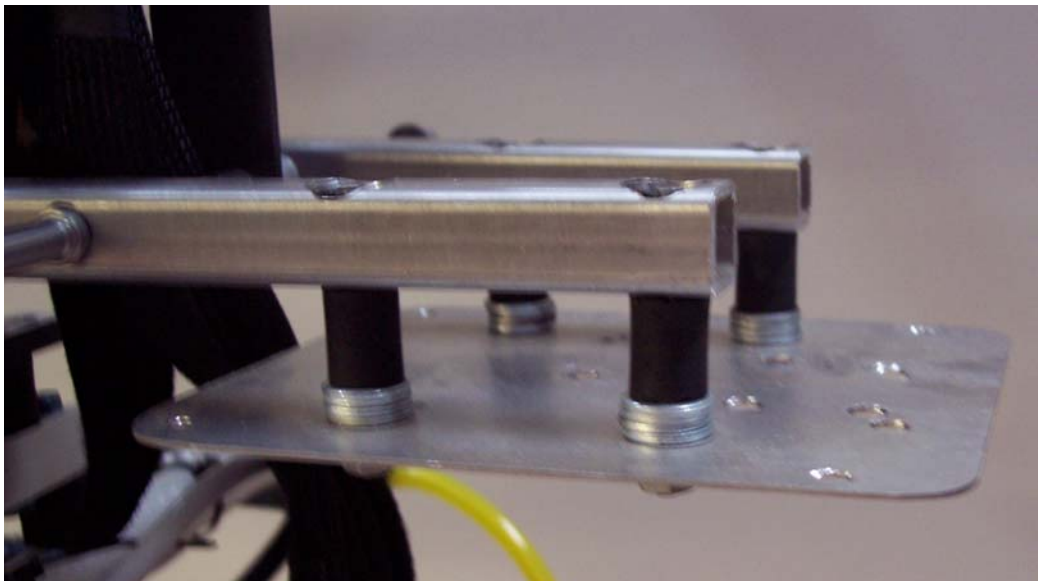

Figure 3.3. Vibration Isolation Mount for Single Board Computer and Power Distribution

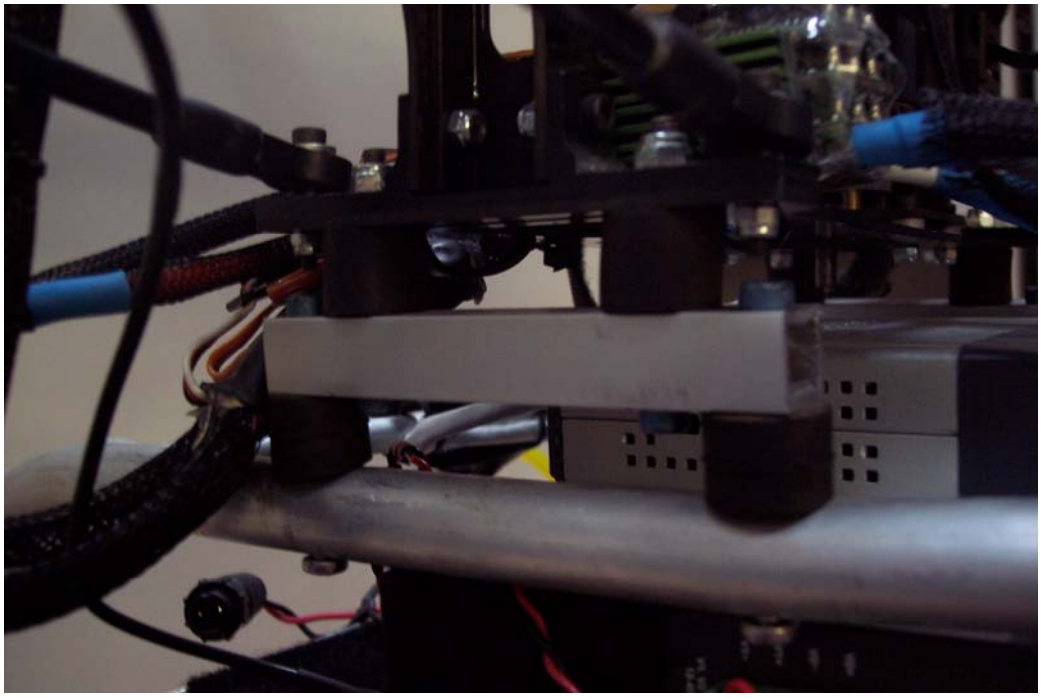

Figure 3.4. Vibration Isolation for the Landing Gear of the SR-20. The Camera and LIDAR sensor are mounted to the Landing Gear.

With all the necessary hardware mounted, the next step is to test the electronics to ensure the power scheme, wiring and network components are functioning properly. The initial concept was to use a spare 12 V output from a small DC-DC board already on the UAV. After brief testing, this was determined to draw too much current from the board,

and cause the onboard wireless network to shut off due to low voltage. To fix this problem, a small, 2-cell, 7.4 V, 5000 mAh lithium polymer battery has been added to the UAV. This adds 0.5 pounds to the system weight, but allows for the entire obstacle detection payload to be independent of the power system on the UAV. Once all components were powered, initial tests using a wired Ethernet connection were used to ensure that all components were wired correctly and working. Finally, all UAV components as well as obstacle detection payload components were powered and the wireless network was tested to ensure that adding the payload components had not caused any IP conflicts or other issues. Several ground tests of the camera, LIDAR and flight controller functionality were performed. This was all done to ensure proper operation in flight.

3.2.3. Ground Station

The purpose of the ground station is to display the available sensor information in a way that enhances the situational awareness of the operator to the point that the mission can be successfully completed. As mentioned before, in addition to the LIDAR information, the operator will have access to a downward facing video stream updating at six frames per second. This adds another feature that requires the attention of the operator for successful navigation. An additional feature to aid in navigation of the UAV is a nearest obstacle indicator. Based on the collected LIDAR data as well as the profile of the UAV, nearest obstacle indicators determine the nearest obstacles to the UAV in front, below, and to the left and right. Although this information can be gathered from the three-dimensional display of the LIDAR data, it allows for quick judgment by the operator in determining immediate collision threats.

To display all this data in a manner that allows for the greatest situational awareness while improving operator performance, dual LCD monitors handle the display of all the information mentioned above, with one monitor providing the video display and the other displaying the three-dimensional LIDAR data plot as well as the nearest obstacle information. There are many options for displaying and orienting display data, and this will be evaluated through a user performance study in the following chapter.

3.2.4. Safety and Flight Operations [16]

Safe and successful operation of the UAV requires the operators to follow a well defined procedure before flying. The preflight and startup procedures detailed here take about ten minutes to complete. An emergency stop system and flight logs are also used to keep operation of the UAV safe.

Preflight

Prior to any testing, a preflight inspection is conducted to ensure that all components of the UAV are working and flight-worthy. A preflight document was created to identify all of the inspection processes that must take place prior to a flight; it is not until these tasks are completed that the system is deemed ready for flight. This preflight checklist includes several mechanical tasks such as checking the fuel level, gear mesh, blade grip tightness, servo linkages, and inspection of all bolts. Likewise, there are several electrical tasks as well such as checking all battery voltages, checking all wire connections, and insuring that all electrical components are powering on and communicating properly. If the preflight inspection is successful, then the startup sequence can then be initiated.

Startup Sequence

In addition to the preflight inspection, a strict startup sequence is followed. This sequence is enforced to ensure that every component that is necessary for a successful flight is powered on and functioning properly. The first step within the sequence is to power on the helicopter, electronics box, and communication system. At this point the safety pilot conducts a range check to ensure that the helicopter and emergency stop mechanism are responding appropriately at the maximum range. Meanwhile, the ground station operator powers on the network access point and verifies that the system bridge is connected and communicating. Next, the flight controller and servos are powered on. Once powered, the ground station operator connects to the flight controller and verifies proper communication. Next, the flight controller magnetometer is calibrated through a series of on-ground rotations and maneuvers. Lastly, all other components (Camera,

sensors, and payload) are powered on and verified for proper communication. If all communication and responses are verified at this point, the system is ready for flight.

Emergency Stop Mechanism

Because this system is developed to be entirely autonomous, a fully independent last resort emergency stop system controlled by a safety pilot is required. The emergency stop system (e-stop), seen in Figure 3.5, is designed such that if triggered it will disconnect the electric motor controller and cut power the motor. It is important to note that this independent e-stop is in addition to the e-stop mechanisms within the flight controller, and the ground station software, and should only be used if all other communication mechanisms fail and the safety pilot cannot recover control. This independent e-stop mechanism is a completely self contained unit which contains an independent battery, RC-receiver, microcontroller, relays, and circuit board. When powered on and triggered the e-stop will receive a signal from the e-stop receiver and fire a set of redundant relays which will disconnect power to the motor. Onboard protection circuitry protects the internal lithium polymer battery from high and low discharge states.

Figure 3.5. Emergency Stop System

Flight Test Log

For every flight, a detailed flight log was recorded in order to document the successful or unsuccessful events. Each flight log contains information regarding the nature of the tests, behavior of the system, weather conditions, any achieved milestones, and any data taken during the flight. This allows us to not only keep a historic record for

the development of the vehicle but also allows us to trouble shoot failure modes and catalog a basis of comparison for any inconsistencies that occur during flight.

Chapter 4: System Evaluation

The final goal of this research is to demonstrate successful obstacle detection and avoidance using this system on board the SR-20. The static performance of the LIDAR-based obstacle detection system has been evaluated at length in Chapter 2. This chapter focuses on the ground based-testing of the system to evaluate the ground station display. Techniques to evaluate user performance to determine the display effectiveness were used. After evaluating different display types, a final ground station was developed based on enhancing user performance as well as on feedback from users. This ground station, in combination with the other system components described in the previous chapter, was used to demonstrate successful flights over a debris field. Details and images from these flights will be discussed at the end of this chapter.

4.1. Ground Based Testing

Based on the customer requirements and mission overview, it is necessary to develop a method for ensuring that this obstacle detection system provides sufficient information to a ground station operator so that they may navigate through obstacle rich environments. Although the system is designed to work on a UAV platform in flight, extensive testing in this arena is difficult due to current limitations in available UAVs. A series of ground-based user performance tests were created to characterize the effectiveness of multiple visual display methods. This is necessary to provide an operator with the level of situational awareness required to complete a simulated UAV descent through an obstacle field. Situational awareness can be described as the perception of the objects in the environment, comprehension of the current situation, and projection of the future status of elements in the environment [17]. Although quantifying the situational awareness provided by each display type is a vague task, there are many methods to quantify the user performance. The following section will focus on the design of the experiment as well as a summary of the results.

4.1.1. Design of the User Performance Evaluation

The current proposed obstacle detection system provides the user with two kinds of visual feedback that may be used to detect and avoid obstacles. The first is the LIDAR-based system and the second is a downward facing camera. The goal of the experiment is to quantify how each system individually, as well as in combination, allow an operator to navigate a UAV. To accomplish this task, a subject-based experiment has been developed in accordance with the Virginia Tech regulations on human subjects research and approved by the Institutional Review Board at Virginia Tech. The approved forms for human subjects research can be found in Appendix B.

A pool of participants with knowledge of UAVs was asked to navigate a simulated obstacle field using the obstacle detection ground station. These subjects were all students ranging in age from 21 to 27 years of age, with the average being 22 years old. The obstacle field, seen in Figure 4.1, incorporates objects of the same size and

material as those of a potential urban environment. The obstacle detection system was mounted on a rolling cart to simulate a vehicle. The subjects were given some combination of available technologies, and asked to navigate the simulated vehicle to 1 meter away from an item of interest seen in the picture below as the orange box mounted on the wall.

Figure 4.1. One of the Simulated Obstacle Fields for User Performance Evaluations

Prior to any attempted navigation, subjects were given an overview of the technologies as well as a mission briefing. After allowing the subjects to become familiar with the software, the mission began. Subjects had a computer dedicated to the obstacle detection system seen in Figure 3.2, and were seated next to a simulated UAV operator. This is how the system currently works for flight operations. The subject was told the UAV was at the starting location, and then their tactical descents began. Subjects used the obstacle detection software to determine their next desired movement of the

vehicle and would then tell the move to the UAV operator. Subjects were allowed to move the simulated UAV in steps as small as 0.25 meters and could give combinations of commands if they wished. The UAV operator would then move the simulated vehicle, and inform the subject they were ready for another movement. This process continued until the subject reached the target location or came into contact with an obstacle, causing a crash.

Figure 4.2. Obstacle Ground Station Computer for User Performance Evaluations.

Using the two monitor system shown above, users had the camera display on the left and the LIDAR display on the right. For the same obstacle scene, the image from the camera as well as the LIDAR display can be seen in Figure 4.3 and Figure 4.4. There are some very important differences between the two displays. The camera, as discussed in Chapter 3, is updating at 6 frames per second continuously during the simulation while the LIDAR display updates only after an entire scan is complete. Additionally, it should be noted that the LIDAR display can be manipulated by rotation or zoom, allowing the user to interact with the software and view obstacles from different angles.

Figure 4.3. Camera display for Obstacle Field Navigation

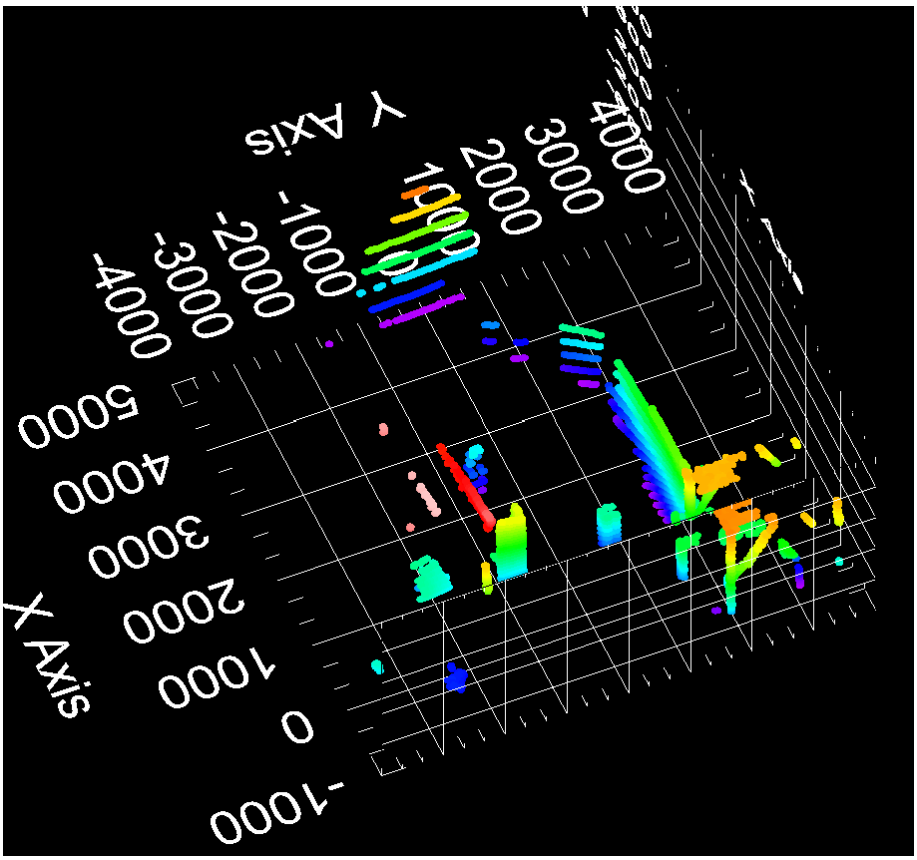

Figure 4.4. LIDAR Display for Obstacle Field Navigation

For each simulated descent by a subject, several pieces of data were collected. For any movement command, the direction and distance were recorded, as well as the time it took the subject to determine this movement once they received obstacle data. This takes out the additional time due to the LIDAR scan and only evaluates the time it took the subject to locate obstacles and make movement decisions. From these pieces of data, it is possible to evaluate and compare each display type based on the overall success rates, average time to determine a vehicle movement, average distance moved and total time to complete the mission.

4.1.2. Results from the User Performance Evaluations

Following the description of the user performance evaluation outline above, subjects volunteered time to help participate in the experiment to evaluate the obstacle detection ground station display. Subjects were randomly given one of the three technology modes for any given attempt. The camera, LIDAR, and the combination of both were each used 10 times in attempted navigations of the obstacle course. From each of these attempts, quantitative as well as qualitative data was collected. The first piece of this data that will be discussed is the completion percentages. Seen in Figure 4.5, it is clear that subjects using the LIDAR display with or without the camera were much more successful than those using the camera. Subjects using only the camera and colliding with obstacles always did so with the edges of the vehicle. When asked about their difficulties with the camera, the most common response from subjects was the lack of peripheral view leading to unknown locations of obstacles once they passed from view. The lack of forward depth perception was less of an issue, and no collisions resulted with an obstacle directly in front of the camera. The collisions that occurred when subjects were only given the LIDAR most commonly occurred due to the users not estimating the size of the vehicle correctly. In all crashes, subjects correctly identified the obstacles but made incorrect movements. The failures when users were given both systems to avoid obstacles came from a combination of reasons. In one of the cases, the user made a quick judgment based on the camera view only, not using the LIDAR display, and collided with an obstacle that was just out of the cameras field of view. The other cases were similar to

the failures with the LIDAR display alone, where operators correctly identified obstacles but made incorrect judgments on how to avoid them.

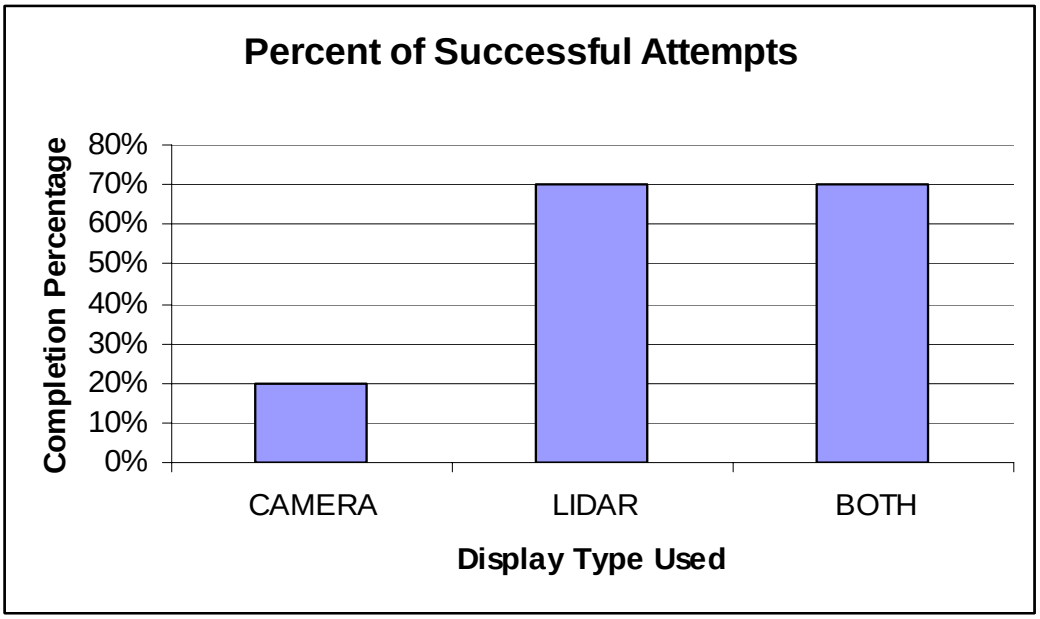

Figure 4.5. Graph of the Successful Navigational Attempts of Users.

Although the overall success of the system is extremely important, other factors weigh into the performance of the display. One way to evaluate how well the systems allow the users to perceive the obstacles around them is to look at the average step size used in navigation. Seen below, the average step size for the LIDAR and the combination of LIDAR and camera were both just less than 1 meter per step while the average movement with the camera alone was 0.65 meters. According to subjects, this was because of the lack of depth information with the camera, resulting in users only being comfortable with smaller movements. Subjects noted that the accurate distance measurements in the LIDAR display allowed for much larger and more confident movements of the vehicle.

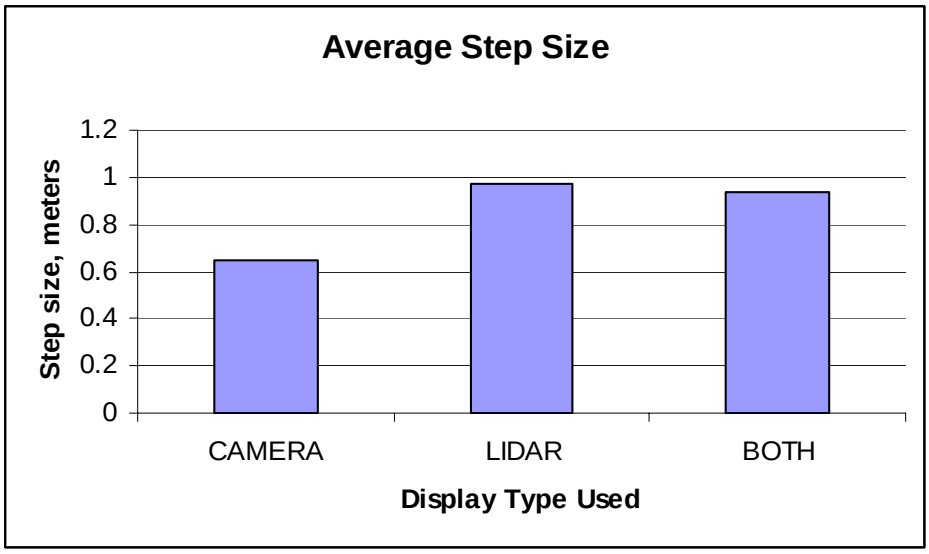

Figure 4.6. Average Step Size for Each Display Type during the User Performance Evaluations.

Related directly to the average step size for each technology is the number of steps required to complete the course. The smaller the step size the ground station operator was comfortable with, the more movements that would be required to reach the target location. Although this was less important for this user performance evaluation, in a real world application, increasing the number of movements of the UAV would increase the workload of the UAV operator.

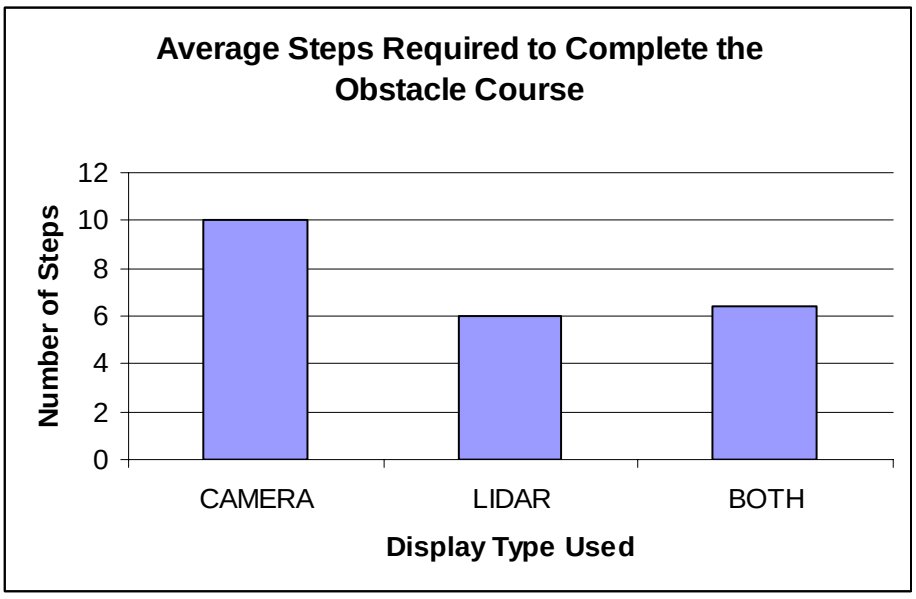

Figure 4.7. Average Number of Steps Required for Users to Successfully Navigate the Obstacle Course.

In any situation involving UAVs, time is a critical factor when comparing obstacle detection systems. The time required for the LIDAR unit to complete a scan has been characterized in Chapter 2, and to add to that, it is necessary to determine the time it would take an operator to make navigational decisions based on the different displays. A graph of the time data collected during the user performance evaluations can be seen in Figure 4.8. The time users required to make a navigational decision using a camera only was 17 seconds less than that for the LIDAR alone and 10 seconds less than both displays being used together. When asked about this trend, users typically stated this was because they were more comfortable with visual images and did not have to manipulate a display to view all potential obstacles. The LIDAR display allows users to view the data from different angles, adding to the decision making time. The slight decrease in time when using both the camera and LIDAR display can be attributed to users feeling more comfortable in identifying obstacles and correlating what they were seeing in both displays to a single perception of the vehicles surroundings.

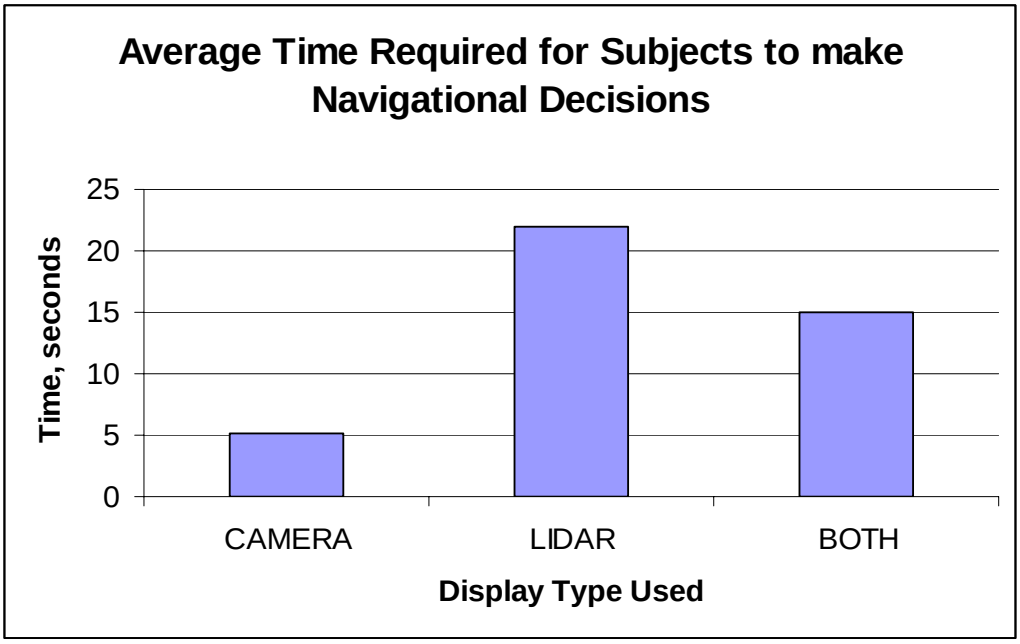

Figure 4.8. Average Time Required for Subjects to Make Navigational Decisions.

Another interesting trend that was seen between the different systems was the number of compound moves made by the users. As stated before, the subjects were

allowed to give multiple movement commands at once if they felt comfortable enough in their perception of the surroundings. Users attempted multiple movements only one time in the 10 navigational attempts using only the camera, compared to 27 times using only the LIDAR and 21 times using both displays. This provides some insight into how well users perceived their surroundings. Users stated their confidence in their vehicle movements increased when the LIDAR display was used to provide accurate distance measurements to obstacles. These compound moves require no additional workload for a UAV operator and allow for greater movements towards the end goal.

Additional user feedback was collected at the end of each navigation attempt. Some of the most common complaints about the LIDAR display were focused on the necessity of a vehicle representation in the three-dimensional plot. Due to limitations in the current software development, there is no immediate solution for this problem. LabView does not have a clean way to integrate vehicle images at this time. However, third party companies do provide a solution for this problem, but these are out of the scope and budget of the research at this time. Another common problem with subjects using the LIDAR display was losing their orientation in the three-dimensional plot. As subjects used the display more during their navigation attempts, they became more comfortable with this. One potential solution would be to incorporate a home button to re-orient the users if they needed it.

4.1.3. Conclusions from the User Performance Evaluations

The data above suggests that the use of a LIDAR system allows for the highest success rate of obstacle course completion. Because of the step by step nature of the commands given to the UAV at this time, access to accurate distance information is critical for successful navigation. Combining a vision system allows users to correlate LIDAR obstacle maps to real world images and results in faster navigational decision making with fewer steps required to complete the course. These are both vital to mission success in reducing the UAV operator workload and limiting the flight time required to navigate through obstacles. Taking into account the user feedback regarding the display, a second generation with additional features could help increase these success rates even

more. Additionally, finding a way to fuse the visual information with the LIDAR data to develop a single display, minimizing the number of windows the operator must use while taking full advantage of the spatial information available [18]. Other studies suggest the use of three-dimensional displays can often confuse users and cause a loss of perspective. One solution to this problem has been demonstrated by the Humans and Automations Lab at Massachusetts Institute of Technology for use with the AAI Shadow UAV, and consisted of two, two-dimensional displays, with one as an overhead view and another as a profile view [19]. Although this display type works well for fixed wing UAVs limited to forward flight, a more advanced version would be required to take advantage of the available degrees of freedom of a VTOL UAV.

4.2. Flight Tests over a Debris Field

To validate the successful development of this obstacle detection system, flights over a debris field simulating an urban site were performed. Prior to this complex flight testing, more simple tests were initially performed. The first of these tests involved mounting the LIDAR directly to the landing gear tray on the SR-20 without the servo control. This still uses the single board computer mounted in its previous discussed location. The purpose of this test was to verify proper function of the LIDAR system onboard the UAV while in flight. With this being the first in flight test, factors such as vibration of the LIDAR sensor and communication link were the primary concerns. With the help of Shane Barnett as the safety pilot, the SR-20 was flown autonomously directly in front of our mock MOUT site in the Plantation Road field. Using the LIDAR system in a single plane, the edges of the window frame as well as the edges of the building were clearly identified. The SR-20 was moved to different heights to verify finding the walls as well as the openings on the front of the building. The image in figure 4.9 was taken during one of these test flights. The SR-20 was hovering fully autonomously less than three meters from the face of the building.

Figure 4.9. Testing of the LIDAR Sensor on the SR-20. This image was taken while flying in front of the mock MOUT site

This test confirmed that the LIDAR unit functioned properly in flight, and also verified that the mounting location would provide sufficient vibration isolation. This also verified the ability of the SR-20 to fly near obstacles and maintain a steady hover. It is important to note this was a very calm day, with winds less than 5 mph and no large gusts. With the success of this test, the next test was to mount to entire obstacle detection payload and test that system. The first flight tests were performed at higher altitude, approximately 15 meters above the ground, to ensure no obstacles or hazards were going to pose an immediate risk. During initial testing, the LIDAR sensor and servomotor worked as expected and scan data was returned to the ground station. The SR-20 was then lowered to approximately 3 meters above some obstacles and a scan was run. The LIDAR system detected the obstacles below the UAV, however it was an extremely gusty day with winds in the 15 mph range, so no quantitative testing could be safely conducted. A picture from the initial day of testing is seen below. It can be seen that the LIDAR sensor is in the middle of scan directly above the obstacles.

Figure 4.10. Flight test of the SR-20 Using the Obstacle Detection Payload above Obstacles

To perform additional tests to verify the ability of the system to detect obstacles in the urban setting, a test site has been secured that has many of the desired objects we would like to be able to detect. The test site, seen above in Figure 4.10 provides a road, several different kinds of cement and metal debris, rebar and a rope used to simulate a power line. Due to mechanical complications with the SR-20 UAV, no further flight tests have been performed at this time. These additional flight tests are still planned once the UAV can be repaired and safe autonomous flight can be resumed. The initial tests showed that the system was working and successfully detecting obstacles in flight.

Chapter 5: Conclusions

As originally stated, the purpose of this research was to design an obstacle detection system to meet the customer requirements for the project. After investigating several potential sensor options, the Hokuyo URG-04LX two-dimensional LIDAR sensor was chosen. This sensor was then paired with a servomotor to produce a system capable of providing 240 degree LIDAR scans at a distance of 5.5 meters from the sensor, and rotating the sensor 130 degrees, to provide a large area of obstacle detection. Using the PC-104 single board computer to provide on-board processing power to control the LIDAR sensor and servomotor, a stand alone obstacle detection system was created. Using LabView software, the on-board control and the ground station display were developed. The final product of the research was a fully functional three-dimensional obstacle detection system that is both compact, light weight, and low power. The system was tested extensively on the ground. Initial aerial tests on the UAV were performed as well.

After developing the obstacle detection system, it was important to ensure characterize the user performance effects of the system for human supervisor control of a UAV. As required by the customer, a human operator must be able to look at the obstacle detection system ground station display and make safe and efficient movements to avoid obstacles while attempting to reach a final goal position for the UAV. Through the use of an approved human subjects experiment, results to determine the user performance impacts of the LIDAR-sensor display were found. In comparison to using only a camera, subjects have the LIDAR display or both the LIDAR and camera display were able to successfully navigate an obstacle course 70% of the time while those using only the camera only had a 20% success rate. Additionally, subjects using the LIDAR display were able to complete the obstacle course in fewer steps than the camera, resulting in fewer UAV movements in a flight scenario.

5.1. Future Work

Although the system is fully functional at the moment and meets the stated customer requirements, there are several improvements that could be made. With regard to the hardware, there is a potential to scale down the on-board computing requirements, potentially to the point of using a small microprocessor rather than a PC-104 computer. This would save weight and reduce power consumption. Increasing scan time would be another desired improvement and could be achieved through the use of a motor with feedback so a faster more fluid scan could be used to take advantage of the sensors 10 Hz scan rate. Software improvements in the on-board system would be based on the available hardware to improve scan times.

In addition to the valuable quantitative results from the human subjects study on user performance, the user feedback provided additional improvements that could be made to the ground station. The most common problem for users was the lack of perception of the vehicle in the three-dimensional plot. Although LabView does not have a clean solution to this problem, third party software is available that provides ways to incorporate three dimensional renderings of the UAV into a three-dimensional obstacle field. As discussed in the conclusions on user performance evaluations, there are many possibilities to further enhance the situational awareness of the operator and allow for more effective supervisory control of the UAV. Additional user performance evaluations would be required to determine the impacts of different displays.

Another area that could be explored to increase the effectiveness of the system would be to add additional autonomy to the system. In "A model for Types and Levels of Human Interaction with Automation," an approach is developed to address the issue of adding autonomy to a system to improve human performance [20]. Seen in Figure 5.1, a model of human information processing is presented, and each stage of can have varying levels of autonomy.

Figure 5.1. Simple four-stage model of human information processing [20]

The stages most applicable for automation in this research would be the decision making. Based on Table 5.1, and given the customer requirements of this project, a low level of automation and decision selection could be implemented. Additional user performance evaluations could be conducted to determine the effectiveness of the automation levels.

Table 5.1. Levels of Automation of Decision and Action Selection [20]

HIGH	10. The computer decides everything, acts autonomously, ignoring the human.
	9. informs the human only if it, the computer, decides to
	8. informs the human only if asked, or
	7. executes automatically, then necessarily informs the human, and
	6. allows the human a restricted time to veto before automatic execution, or
	5. executes that suggestion if the human approves, or
	4. suggests one alternative
	3. narrows the selection down to a few, or
	2. The computer offers a complete set of decision/action alternatives, or
LOW	1. The computer offers no assistance: human must take all decisions and actions.

References

1. T. B. Sheridan, *Telerobotics, automation and human supervisory control*, The MIT Press, Cambridge, Massachusetts, 1992.

2. C. W. Nielson, M. A. Goodrich, and R.W. Ricks, "Ecological Interfaces for Improving Mobile Robotic Teleoperation," *IEEE Transactions on Robotics*, vol. 23, no. 5, pp. 927-941, 2007.

3. D. D. Woods, J. Tittle, M. Feil, and A. Roesler, "Envisioning Human-robot coordination in future operations," *IEEE Transactions on Systems, Man, and Cybernetics*, part C, vol. 34, no. 2, pp. 85-116, 2004.

4. D. Woods and J. Watts, "How not to have to navigate through too many displays," in *Handbook of Human-Computer Interaction*, 2nd ed., M. Helander, T. Landauer, and P. Prabhu, Eds. Amsterdam, The Netherlands: Elsevier Science, 1997, pp. 1177-1201.
5. J. Bouget, "Pyramidal Implementation of the Lucas Kanade Feature Tracker – Description of the algorithm," Intel Corporation, Microprocessor Research Labs.

6. K. Muhlmann, D. Maier, J. Hesser, and R. Manner, "Calculating Dense Disparity Maps from Color Stereo Images, an Efficent Implementation," Proceedings *IEEE Workshop on Stereo and Multi-Baseline Vision*, 2001.

7. Point Grey Research, Available: http://www.ptgrey.com/products/stereo.asp

8. Acroname Robotics, Available: http://acroname.com/robotics/parts/R145-SRF08.html

9. R. R. Murphy, *Introduction to AI Robotics*, The MIT Press, Cambridge, Massachusetts, 2000. pp. 214.

10. D. H. Shim, H. Chung, H. J. Kim, and S. Sastry, "Autonomous Exploration in Unknown Urban Environments for Unmanned Aerial Vehicles," Proceedings *AIAA Guidance, Navigation and Control Conference*, 2005.

11. S. Scherer, S. Singh, L. Chamberlain, and S. Saripalli, "Flying Low and Fast Among Obstacles," Proceedings *IEEE International Conference on Robotics and Automation*, 2007.

12. S. Hrabar, G. S. Sukhatme, P. Corke, et al. "Combined Optic-Flow and Stereo-Based Navigation of Urban Canyons for a UAV," Proceedings *IEEE International Conference on Intelligent Robots and Systems*, 2005.

13. Hokuyo Products, Available: http://www.hokuyo-aut.jp/02sensor/07scanner/urg.html

14. MICRO/SYS Products, Available: http://www.embeddedsys.com/subpages/products/sbc1586.shtml

15. Rotomotion, LLC., Available: http://www.rotomotion.com/prd_UAV_SR20.html

16. S. Barnett, J. Bird, A. Culhane, et al., "Deployable Reconnaissance from a VTOL UAS in Urban Environments," Proceedings *SPIE Conference on Unmanned Systems Technology IX*, 2007.

17. M. R. Endlsey, "Designing for Situational Awareness in Complex System," Proceedings of *The Second International Workshop on Symbiosis of Human, Artifacts and Environment*, Kyoto, Japan, 2001.

18. H. A. Yanco, J. L. Drury, and J. Scholtz, "Beyond usability evaluation: Analysis of human-robot interaction at a major robotics competition," *Journal of Human-Computer Interaction*, vol. 19, no. 1 and 2, pp 117-149, 2004.

19. M. L. Cummings, J. J. Marquez, M. Visser, "Shadow TUAV Single Operator Consolidation: Display Assessment," Humans and Automation Laboratory, Massachusetts Institute of Technology, Dept. Aeronautics and Astronautics, Cambridge, MA, Jan. 2007.

20. R. Parasuraman, T. B. Sheridan, C. D. Wickens, "A Model for Types and Level of Human Interaction with Automation," *IEEE Transactions on System, Man and Cybernetics*, Part A: Systems and Humans, vol. 30, no. 3, pp. 286-297, 2000.

Appendix A: Obstacle Detection System Components

A.1. Power Distribution Board Schematic

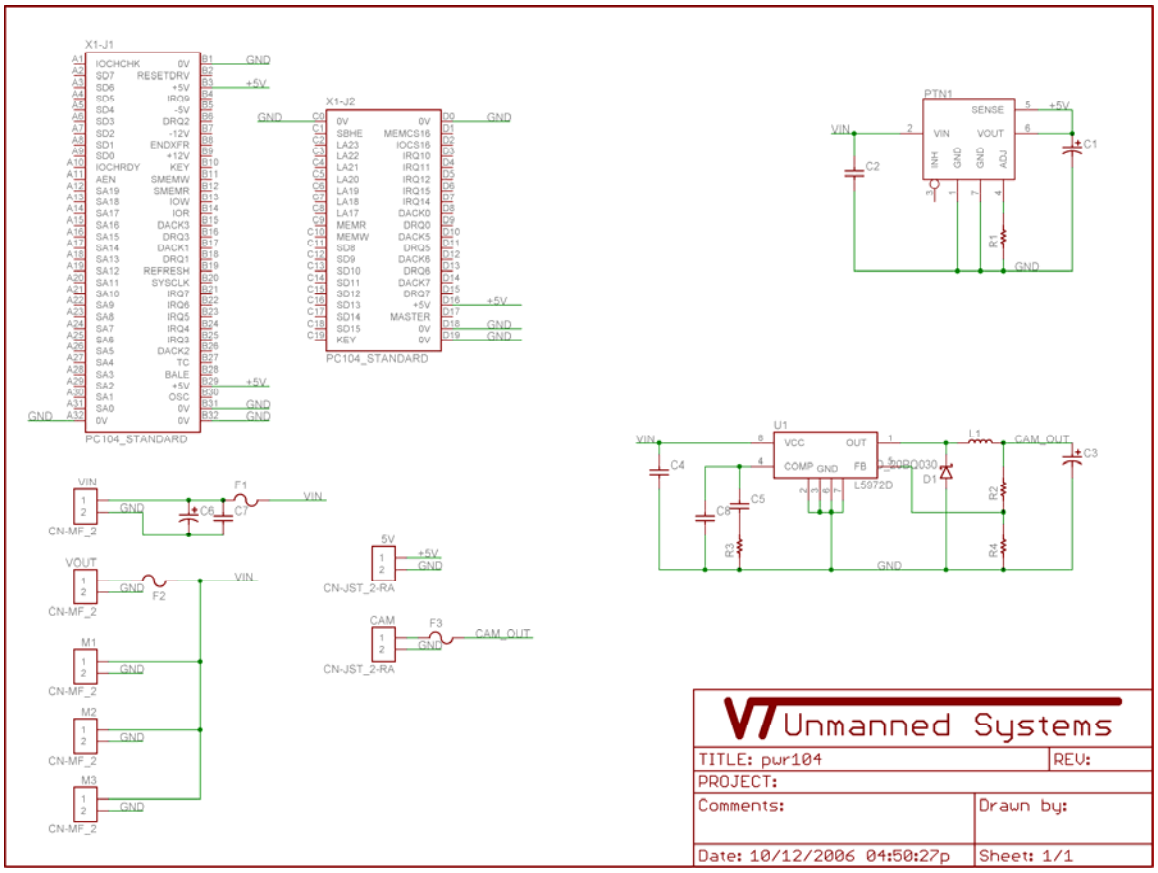

Appendix B: User Performance Evaluations

B.1. User Performance Evaluation Data Collection Sheet

User Performance Evaluation Form for Obstacle Detection Ground Station

Test Administrator: Andrew Culhane, VT Unmanned Systems Lab

Explanation of Test
Part 1: The subject will customize the display settings using a test scene. Questions about preferences will be asked during this process regarding settings and views.

Part 2: Navigation of an obstacle course. During this, notes will be taken regarding the time between movements, successful completion of the course and comments from the subjects.

Part 3: Final feedback. The subject will briefly discuss likes and dislikes of the display system.

Test Data
Subject Number:
Obstacle Course Number:
Display Type Available (circle one): Camera only LIDAR only Both

Part 1: Display Settings and Comments

Part 2:

Movement Number	Time	Safe Move	Comments
1			
2			
3			
4			
5			
6			
7			
8			
9			
10			
11			
12			
13			
14			
15			
16			

Part 3: Final Comments

B.2. Institutional Review Board Approved Forms

VirginiaTech

Office of Research Compliance
Institutional Review Board
2000 Kraft Drive, Suite 2000 (0497)
Blacksburg, Virginia 24061
540/231-4991 Fax 540/231-0959
e-mail moored@vt.edu
www.irb.vt.edu

FWA00000572(expires 1/20/2010)
IRB # is IRB00000667

DATE: November 8, 2007

MEMORANDUM

TO: Kevin Kochersberger
Andrew Culhane

Grant Compared 11/7/07
Approval date: 11/7/2007
Continuing Review Due Date:10/23/2008
Expiration Date: 11/6/2008

FROM: David M. Moore

SUBJECT: **IRB Expedited Approval:** "Evaluation of a Ground Control Station Interface for Autonomous Helicopter Navigation", OSP #415570, IRB # 07-560

This memo is regarding the above-mentioned protocol. The proposed research is eligible for expedited review according to the specifications authorized by 45 CFR 46.110 and 21 CFR 56.110. As Chair of the Virginia Tech Institutional Review Board, I have granted approval to the study for a period of 12 months, effective November 7, 2007.

As an investigator of human subjects, your responsibilities include the following:

1. Report promptly proposed changes in previously approved human subject research activities to the IRB, including changes to your study forms, procedures and investigators, regardless of how minor. The proposed changes must not be initiated without IRB review and approval, except where necessary to eliminate apparent immediate hazards to the subjects.
2. Report promptly to the IRB any injuries or other unanticipated or adverse events involving risks or harms to human research subjects or others.
3. Report promptly to the IRB of the study's closing (i.e., data collecting and data analysis complete at Virginia Tech). If the study is to continue past the expiration date (listed above), investigators must submit a request for continuing review prior to the continuing review due date (listed above). It is the researcher's responsibility to obtained re-approval from the IRB before the study's expiration date.
4. If re-approval is not obtained (unless the study has been reported to the IRB as closed) prior to the expiration date, all activities involving human subjects and data analysis must cease immediately, except where necessary to eliminate apparent immediate hazards to the subjects.

Important:
If you are conducting **federally funded non-exempt research**, this approval letter must state that the IRB has compared the OSP grant application and IRB application and found the documents to be consistent. Otherwise, this approval letter is invalid for OSP to release funds. Visit our website at http://www.irb.vt.edu/pages/newstudy.htm#OSP for further information.

As indicated on the IRB application, this study is receiving federal funds. The approved IRB application has been compared to the OSP proposal listed above and found to be consistent. Funds involving procedures relating to human subjects may be released. Visit our website at www.irb.vt.edu for further information

cc: File
OSP

VIRGINIA POLYTECHINC INSTITUTE AND STATE UNIVERSITY

Informed Consent for Participants
in Research Projects Involving Human Subjects

Evaluation of a Ground Control Station Interface for Autonomous Helicopter Navigation

Investigators: Dr. Kevin Kochersberger, Andrew Culhane

I. Purpose of this Research

The goal of this research is to evaluate three different display types for their effectiveness in simulated navigation of a UAV. Subjects will have a basic knowledge of the uses and operations of UAVs.

II. Procedures

Subjects will be given a brief explanation of the mission scenario as well as how to operate the ground station interface. Subjects will then attempt to use the specified ground station interface to navigate a short obstacle course simulating an operating environment for a UAV. The research will take place in the Unmanned Systems Lab at Plantation Road. The performance metrics that will be recorded are time per command given, commands given, and total time.

III. Risks

The risks involved in this research will be similar to those of sitting at a computer for no more than 30 minutes. All efforts will be made to ensure operator comfort during the test.

IV. Benefits

The benefit of this research is in evaluating the different display types for UAV navigation in order to increase the operational range of current UAV technology.

V. Extent of Anonymity

All subjects will be identified in the study using only a number. No personal data will be recorded. Photographs or video may be taken, and those will be stored on a secure computer at the Unmanned Systems Lab. If any of these images are used in publications or reports, the participant will be asked for consent and not identified in the document.

VI. Compensation

Participants will not be compensated for this research.

VT IRB – This document is valid from 7 November 2007 – 6 November 2008

VII. Freedom to Withdraw

Subjects are free to withdraw from this study at any time without penalty. Subjects are free not to answer any questions of respond to experimental situations that they choose without penalty.

VIII. Subjects Responsibilities

I voluntarily agree to participate in this study. I have the following responsibilities:

Participation in the evaluation of the Ground Station Interface

IX. Subject's Permission

I have read the Consent Form and conditions of this project. I have had all my questions answered. I hereby acknowledge the above and give my voluntary consent:

Subject Signature_____ Date_____

Should I have any pertinent questions about this research or its conduct, and research subject's right, and whom to contact in the event of a research-related injury to the subject, I may contact:

Investigator:

Andrew Culhane	540-231-0902	aculhane@vt.edu

Faculty Advisor:

Dr. Kevin Kochersberger	540-231-5589	kbk@vt.edu

Department Head:

Dr. Kenneth Ball	540-231-6661	ball@vt.edu

David M. Moore 540-231-4991 moored@vt.edu
Chair, Virginia Tech Institutional Review
Board for the Protection of Human Subjects
Office of Research Compliance
2000 Kraft Drive, Suite 2000 (0497)
Blacksburg, VA 24060

VT IRB – This document is valid from 7 November 2007 – 6 November 2008